

**HYPOTHESIS****SUBJECT COLLECTION: EXPLORING THE NUCLEUS**

# Specialization of nuclear membrane in eukaryotes

Yuki Hara

**ABSTRACT**

The size of the intracellular structure that encloses genomic DNA – known as the nucleus in eukaryotes and nucleoid in prokaryotes – is believed to scale according to cell size and genomic content inside them across the tree of life. However, an actual scaling relationship remains largely unexplored across eukaryotic species. Here, I collected a large dataset of nuclear and cell volumes in diverse species across different phyla, including some prokaryotes, from the published literature and assessed the scaling relationship. Although entire inter-species data showed that nuclear volume correlates with cell volume, the quantitative scaling property exhibited differences among prokaryotes, unicellular eukaryotes and multicellular eukaryotes. Additionally, the nuclear volume correlates with genomic content inside the nucleus of multicellular eukaryotes but not of prokaryotes and unicellular eukaryotes. In this Hypothesis, I, thus, propose that the basic concept of nuclear-size scaling is conserved across eukaryotes; however, structural and mechanical properties of nuclear membranes and chromatin can result in different scaling relationships of nuclear volume to cell volume and genomic content among species. In particular, eukaryote-specific properties of the nuclear membrane may contribute to the extreme flexibility of nuclear size with regard to DNA density inside the nucleus.

**KEY WORDS:** Intracellular size scaling, Allometry, Nuclear size, Cell size, Genomic content

**Introduction**

Eukaryotes have acquired diverse organelles during their long evolutionary history. In each species, the cells can alter the morphology of the organelle to adjust the function by reflecting on drastic changes in the surrounding environments. For instance, the size of organelles varies among species and is dynamically altered throughout the cell cycle, as well as during development and differentiation in individual species (Chang and Marshall, 2017; Wesley et al., 2020). Considering the diversity in organelle size, there is a general principle of a scaling relationship inside the cell between the size of an organelle and the cell. Although scaling analyses have been often utilized at the level of body size, ‘intracellular size scaling’ has been found for certain organelles (including membrane-less structures), such as the nucleus, centrosome, mitotic spindle, mitochondria, cilium, chloroplast, and so on (Hara and Kimura, 2011; Marshall, 2015; Okie et al., 2016). In general, the total organelle size (including changes in the number of some organelles, e.g. mitochondria and chloroplasts) increases with the cell size. In particular, the nucleus – which contains genomic DNA in all eukaryotes and has a pivotal role in

cellular function – has been of interest for over a century for analyzing intracellular size-scaling relationships (Hertwig, 1903; Boveri, 1905; Conklin, 1912). On the basis of microscopic observations of the nucleus within several eukaryotes, including unicellular eukaryotes, the nuclear-to-cytoplasmic (N/C) volume ratio, or allometric scaling function, which is given as  $NV \sim CV^A$  – where  $NV$  is the nuclear volume,  $CV$  is the cell (or cytoplasmic) volume and  $A$  is a scaling exponent – has been analyzed (Neumann and Nurse, 2007; Jorgensen et al., 2007; Price et al., 1973; Šimová and Herben, 2012; Jevtić and Levy, 2015; Tsichlaki and FitzHarris, 2016; Uppaluri et al., 2016). When nuclear size is compared with cell size in species within a single phylum or within limited types of cell in individual species, the N/C volume ratio is generally constant, regardless of any observed variation in cell size. This means that the scaling exponent  $A$  is  $\sim 1$  and that nuclear size exhibits a linear proportional relationship with cell size (Neumann and Nurse, 2007; Jorgensen et al., 2007; Price et al., 1973; Šimová and Herben, 2012; Jevtić and Levy, 2015). On the basis of these experimental evidences, the scaling relationship between the nucleus and cell sizes has been assumed to be conserved across eukaryotes.

The size of the nucleus plays a significant role in the regulation of intranuclear DNA functions, including transcription and replication. Indeed, an abnormality in nuclear size is often observed in cancer cells, and manipulation of nuclear size by genetic perturbation of nuclear size determinants correlates with failures in development and cellular function, including transcriptional activity (Jevtić and Levy, 2015; Edens et al., 2013). Furthermore, the size of the condensed chromosomes in the mitotic spindle, which impacts the correct partitioning of chromatids to daughter cells during mitosis (Schubert and Oud, 1997; Neurohr et al., 2011), can be altered when the size of the nucleus is manipulated experimentally in embryos *in vivo* (Hara et al., 2013; Ladouceur et al., 2015). Previous biochemical analyses have unraveled the molecular mechanisms that control nuclear size and N/C volume ratio in the limited model organisms. Most of the proposed mechanisms share a common concept that involves the availability of nuclear-size determinants in the cytoplasm. These determinants have been identified as nuclear lamina constituents and regulators of importing these constituents into the nucleus (Levy and Heald, 2010; Brownlee and Heald, 2019; Edens et al., 2017; Jevtić et al., 2015), lipid membranes supplied from the endoplasmic reticulum and synthesized in cytoplasm (Hara and Merten, 2015; Kume et al., 2019), as well as other cytoplasmic factors (Kume et al., 2017; Walters et al., 2019; Cantwell and Nurse, 2019a). With this concept, in which the amount of determinants is limited, it is possible to explain the general scaling relationship of nuclear size and its nuclear expanding speed with increasing cytoplasmic volume (Goehring and Hyman, 2012).

In addition to the nuclear-size scaling with cell size, there is another size-scaling relationship with regard to the genomic content within the nucleus. The mass of DNA, corresponding to the genome size inside the nucleus, exhibits tremendous variation among eukaryotes,

Evolutionary Cell Biology Laboratory, Faculty of Science, Yamaguchi University, Yoshida 1677-1, Yamaguchi city 753-8512, Japan.

Author for correspondence (yukihara@yamaguchi-u.ac.jp)

ID Y.H., 0000-0001-6647-6595

as e.g. between *Xenopus laevis* (~3 Gb) and fission yeast *Schizosaccharomyces pombe* (~12 Mb), implying that the nuclear size correlates with the enclosed DNA mass. Indeed, it has long been observed that, between different species, nuclear size correlates with nuclear genomic content (Price et al., 1973; Šimová and Herben, 2012; Cavalier-Smith, 1985; Gregory, 2001; Vinogradov and Anatskaya, 2006), as well as between cells of different DNA ploidy within individual species (Fankhauser, 1945; Robinson et al., 2018; Jevtić and Levy, 2017; Gillooly et al., 2015). Biochemical approaches using a cell-free system of *X. laevis* egg extracts have determined that DNA and chromatin interact with the nuclear lamina constituents, nuclear pore complexes in some eukaryotes, as well as with membrane lipids to promote initial nucleus formation immediately after chromosome segregation at the telophase (Ulbert et al., 2006; Anderson and Hetzer, 2007; Zierhut et al., 2014). Because the DNA structure is common among eukaryotes, the scaling of nuclear size with genomic content is possibly conserved across species. However, the experimental manipulation of cell size without any change in DNA ploidy can alter nuclear size in *X. laevis* egg extracts (Levy and Heald, 2010; Hara and Merten, 2015). Additionally, nuclear volume increases steadily and maintains the N/C volume ratio when DNA content suddenly doubles upon DNA replication during interphase in individual cells of yeast *in vivo* and human cell cultures (Neumann and Nurse, 2007; Jorgensen et al., 2007; Maeshima et al., 2010). These evidences suggest that cell size, rather than genomic content, directly determines nuclear size (Levy and Heald, 2012; Edens et al., 2013; Cantwell and Nurse, 2019b). Owing to these controversial evidences that, in certain cases, reveal a lesser contribution of genomic content towards nuclear size determination, their underlying mechanisms have not been analyzed systematically among a wide range of eukaryotes.

Considering the relationship between nuclear size and cellular function, the underlying mechanisms of nuclear-size scaling are presumed to be fundamental in the cell organization of all eukaryotes. Despite this being assumed to be conserved among eukaryotes, this phenomenon is still debatable. In fact, as judged from the published experimental studies, the absolute values of the N/C volume ratio appear to be different among species; compare, for instance, budding yeast *Saccharomyces cerevisiae* (~0.1; Jorgensen et al., 2007), *S. pombe* (~0.08; Neumann and Nurse, 2007), developed embryos in *X. laevis* (~0.04; Jevtić and Levy, 2015) and herbaceous angiosperms (~0.2; Milo and Philips, 2016). Additionally, when calculating the scaling exponent of nuclear size to cell size for different cell types from the same organism, different values are obtained; i.e. ~0.4 for intestinal cells (Uppaluri et al., 2016) and ~0.63 for embryonic cells (Arata et al., 2015) of *Caenorhabditis elegans*. The scaling exponent of DNA ploidy to cell size is distinct when measured in different cell types from the same organism, or when measured in the same cell type (traditionally red blood cells) across different organisms (Gillooly et al., 2015). Therefore, the ‘phylogenetic’ interspecies as well as ‘ontogenetic’ intraspecies comparisons of nuclear size could help us understand biological and evolutionary significance of nuclear-size scaling across species with regard to diverse lifestyles, differentiation and development status in individual species and intracellular environments.

In this Hypothesis, I begin with a meta-analysis of the scaling relationship between nuclear size and cell size across species, over a variation of phyla, kingdoms and domains, and continue with the same analysis for nuclear size and genomic content. On the basis of the results obtained, I propose how the evolution of nuclear structures across the tree of life can be explained from the perspective of size-scaling relationship and nuclear membrane composition.

### Scaling of nuclear volume with cell volume

I collected data of nuclear and cell volumes across various phyla in eukaryotes, including 143 species and 667 cell types, and categorized them based on trophic lifestyle and cellularity as multicellular heterotrophic, multicellular phototrophic or unicellular eukaryotes (original data are shown in Tables S1 and S2). In each category, the nuclear volume was plotted against the cell volume in a log-log plot and fitted with the power-law regression line as  $NV=B\times CV^A$ , where  $NV$  and  $CV$  are the nuclear and cell volumes, respectively, and  $A$  and  $B$  are constants ( $A$  is the scaling exponent; Fig. 1A). Especially for blastomeres from early embryonic development in metazoans (before timing of the mid-blastula transition when synchronous rapid cell division is completed), nuclear volumes are relatively smaller

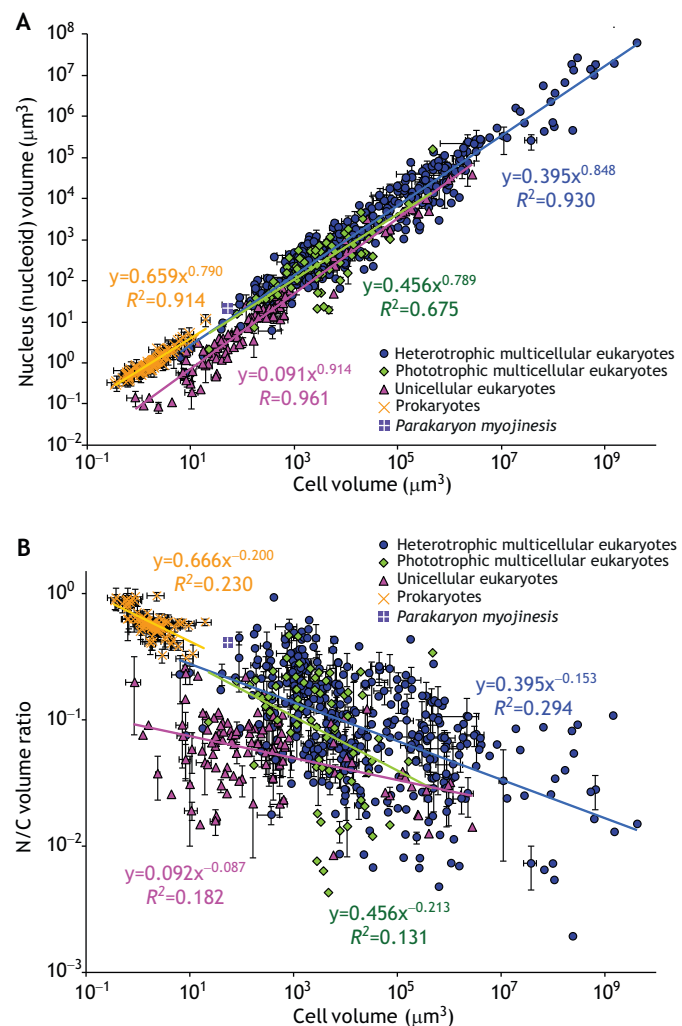


**Fig. 1. Size scaling of nucleus over cell volume among species, in unicellular and multicellular eukaryotes as well as prokaryotes.** (A) Size scaling of nucleus over cell volume for different cell types (excluding early embryonic development in multicellular organisms). Datasets were categorized into heterotrophic multicellular eukaryotes (blue circles,  $n=395$ ), phototrophic multicellular eukaryotes (green diamonds,  $n=75$ ), unicellular eukaryotes (pink triangles,  $n=112$ ), prokaryotes (orange crosses,  $n=107$ ) and *Parakaryon myojinesis* (purple cross,  $n=1$ ). Datasets are represented as the mean ( $\pm$ s.d.) of each sample and fitted with a power-law regression line in each category. The equation and coefficient of determination ( $R^2$ ) are indicated. (B) Nuclear-to-cytoplasmic (N/C) volume ratios are not constant among species. N/C volume ratios are plotted against cell volumes. All datasets shown in this figure and of the individual measurement are available in Tables S1 and S2, respectively.

compared to those in non-embryonic cells (Fig. S1). This is possibly because the nucleus typically cannot expand until it reaches a plateau size within the extremely short duration of interphase (Jevtić and Levy, 2015; Levy and Heald, 2010). To rule out cases of immature nuclear expansion, I henceforth excluded the data for early embryos in metazoans before putative mid-blastula transition from the plots (Fig. 1A). From this plot, the scaling exponents ( $A$  values) were  $0.848 \pm 0.012$  ( $P < 0.001$ ,  $R^2 = 0.930$ ) for multicellular heterotrophs,  $0.789 \pm 0.067$  ( $P < 0.001$ ,  $R^2 = 0.675$ ) for multicellular phototrophs and  $0.914 \pm 0.018$  ( $P < 0.001$ ,  $R^2 = 0.961$ ) for unicellular eukaryotes. In unicellular eukaryotes,  $A$  value is close to 1, corresponding to a proportional interspecies relationship, and consistent with the observed constant values for the N/C volume ratio obtained from individual yeast species when the cell volumes were altered experimentally (Neumann and Nurse, 2007; Jorgensen et al., 2007). Nonetheless, the estimated scaling exponents in all categories (multicellular heterotrophs, multicellular phototrophs, and unicellular eukaryotes) exhibited hypoallometry ( $A < 1$ ), especially in multicellular eukaryotes (Fig. 1A). Interestingly, the inter-species scaling exponents in heterotrophic and phototrophic multicellular eukaryotes revealed similar values, suggesting that the mechanisms that underlie size scaling and nuclear structures are conserved among them. Furthermore, the hypoallometric scaling relationship implies that nuclear volume is not merely controlled by cell volume. In agreement with this notion, a recent analysis suggested a contribution of the plasma membrane in altering the availability of nuclear constituents (Brownlee and Heald, 2019). Importin  $\alpha$  – which controls the import of nuclear-size determinants, such as lamin, from the cytoplasm to the nucleus – can bind to the plasma membrane, thus, causing a reduction in the amount of available importin  $\alpha$  in the cytoplasm, which, in turn, results in the control of nuclear size in a manner that is dependent on the cell surface-area (Brownlee and Heald, 2019). This suggests that nuclear volume is, at least partially, determined by cell-surface area and not cell volume. In this case, as the surface area increases at a slower rate than the volume, the correlation between nuclear size and cell volume is expected to yield a slope of  $<1$ , indicating hypoallometry. Given that the genes encoding lamin are conserved only in metazoans and in some plants (Mans et al., 2004; Ciska and Moreno Díaz de la Espina, 2014), this might give rise to the observed reduction in the scaling exponent against cell volume, especially in multicellular eukaryotes. It should be noticed that the coefficient of determination ( $R^2$ ) obtained from the data of phototrophic multicellular eukaryotes was smaller than for others. This might be because the collected data exhibited considerable fluctuation regarding cell size owing to the presence of vacuoles of varying size.

A recent study has analyzed the scaling of inter- and intra-species nucleoid sizes with cell size and genomic content among prokaryotes (Gray et al., 2019), and its data, referring to 37 species and 111 growth conditions, are included in the plots for eukaryotes (Fig. 1A). The nuclear volume in prokaryotes correlates with cell volume and revealed a hypoallometric scaling with cell volume ( $A = 0.790 \pm 0.024$ ;  $P < 0.001$ ,  $R^2 = 0.914$ ), as previously reported (Gray et al., 2019). Interestingly, although the nucleoid volumes were relatively larger than the nuclear volumes within unicellular eukaryotes (when comparing the data that exhibit the corresponding cell volumes), the estimated scaling exponent in prokaryotes did not change substantially (Fig. 1A). This prokaryote-specific size-scaling property might have been due to absence of a nuclear membrane. Since the nucleoid volume is defined by the region that is occupied with chromosomes, a difference in nucleoid volume means a difference in density and distribution of

chromosomes. A high density of chromosomes, corresponding to a low ratio of nucleoid to cell volume, promotes free diffusion of macromolecules, such as ribosomes, within prokaryotic cells (Gray et al., 2019). By contrast, macromolecular crowding in the cytoplasm might affect the distribution of chromosomes and the occupied space of chromosomes. From the viewpoint of eukaryotes, the nuclear membrane is likely to constrain the cytoplasmic space for genomic activity, such as transcription and replication, to interrupt the effects of macromolecules crowding in the cytoplasm.

This observed hypoallometric scaling relationship between nuclear volume and cell size invokes a negative correlation of N/C volume ratio with the cell volume in each eukaryotic category and prokaryotes. When the calculated N/C volume ratios are plotted against cell volume, the N/C volume ratio indicates weak negative correlation with the cell volume for each category (Fig. 1B). Additionally, the variations in N/C volume ratios are less than one order of magnitude, and between  $\sim 0.3$  and  $\sim 0.9$  in prokaryotes; this variation is substantially smaller than the two orders of magnitude observed in multicellular eukaryotes, i.e. between  $\sim 0.5$  and  $\sim 0.005$  (Fig. 1B, spreading at longitudinal axis). This suggests that eukaryotes have greater flexibility with regard to how their nuclear sizes vary relative to their cell volumes as compared to prokaryotic nucleoids. Interestingly, the microorganism *Parakaryon myojinesis*, which is found in the deep sea, exhibits unique intermediate properties that lie between those of eukaryotes and prokaryotes; moreover, it has a nucleoid that is wrapped with a single membrane containing some gaps (Yamaguchi et al., 2012). The data for the size-scaling relationship of *P. myojinesis* appear to be located on the extended regression lines from the prokaryotic data (Fig. 1) and exhibits an N/C volume ratio of 0.408 (Yamaguchi et al., 2012). This suggests that the *P. myojinesis* nucleoid can be classified as a ‘prokaryotic’ nucleoid in terms of size scaling. The discovery of other, yet unknown, species related to *P. myojinesis*, which have a single nuclear membrane without any gaps, and the analysis of their scaling relationship to the cell volume would offer interesting insights into the evolution of eukaryotes from the perspective of nuclear-size scaling.

### Scaling of nuclear volume with genomic content

As discussed above, the observed inter-species diversity in N/C volume ratios implies a contribution of genomic content to nuclear volume, which is intrinsically different among species. By using the available data on genome size (Table S1), I plotted the nuclear volume against genomic content inside the cell and estimated the inter-species scaling relationship as  $NV = B' \times GC^{A'}$ , where  $GC$  is the genomic content (Fig. 2A).

For eukaryotes, the estimated value for the scaling exponent was  $A' > 0$ , although for prokaryotes it was  $A' \approx 0$ , as reported previously (Gray et al., 2019). Although positive values of scaling exponents were observed for eukaryotes, regression analysis revealed a very weak correlation between  $GC$  and  $NV$  in each multicellular ( $R^2 = 0.031$ ) and unicellular eukaryote ( $R^2 = 0.032$ ) (Fig. 2A). This is likely to be caused by the extensive variations in the observed nuclear volumes, such as those determined even within one species having the same genomic content. Therefore, to reduce the effect of nuclear size variation in individual species, the female gamete – i.e. a fully-grown oocyte – of metazoan species was chosen as a representative for multicellular eukaryotes; for unicellular organisms, a cell under typical growth conditions was selected. Although oocytes have characteristics that distinguish them from somatic cells (such as containing yolk), the fact that the expanding nuclear volume plateaus throughout the extremely long interphase during oogenesis is a common feature of oocytes in multicellular

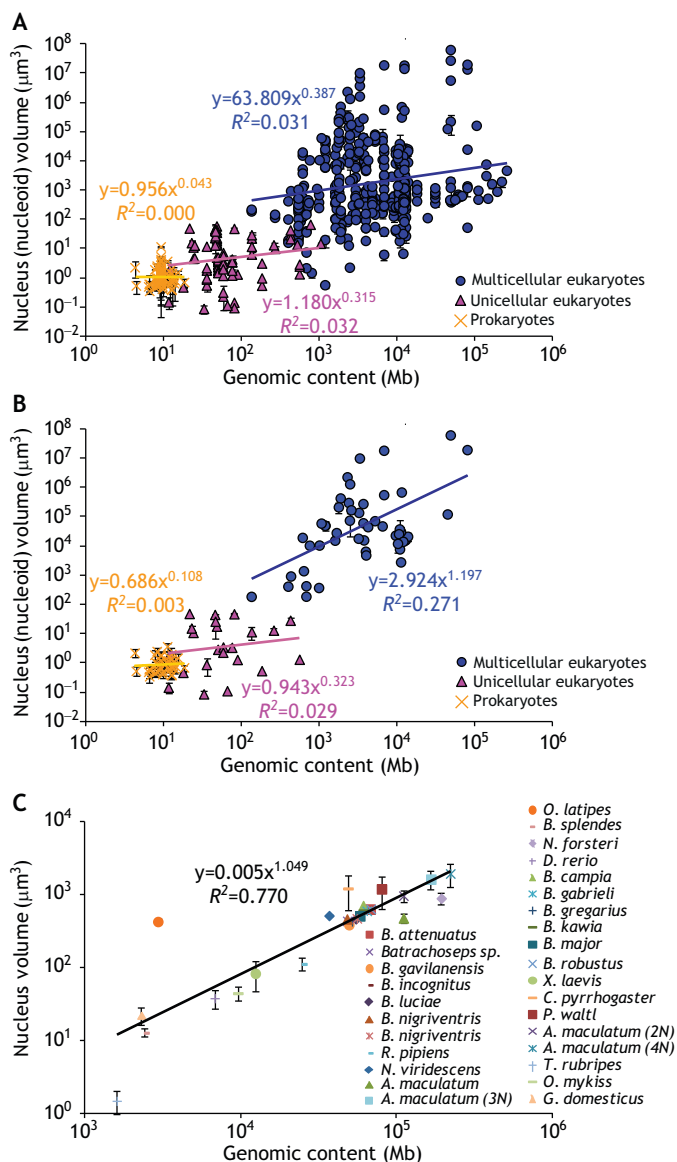


**Fig. 2. Size scaling of nucleus volume over genomic content is only detected in multicellular eukaryotic species.** (A) Size scaling of nucleus volume over genomic content for different cell types (excluding during early embryonic development in multicellular organisms). As before, data were categorized into multicellular eukaryotes (blue circles,  $n=470$ ), unicellular eukaryotes (pink triangles,  $n=84$ ), and prokaryotes (orange crosses,  $n=106$ ). Datasets are represented as the mean ( $\pm$ s.d.) of each sample and fitted with a power-law regression line in each category. The equation and coefficient of determination ( $R^2$ ) are indicated. (B) Size scaling of nucleus volume over genomic content in female gametes (a fully-grown oocyte) of multicellular metazoan organisms (blue;  $n=52$ ), as well as unicellular organisms under normal growth conditions (eukaryotes: pink,  $n=21$ ; prokaryotes: orange,  $n=40$ ). Each species with each DNA ploidy is represented by one symbol with error bar ( $\pm$ s.d.). (C) Size scaling of nucleus volume over genomic content for nucleated erythrocytes in metazoan species ( $n=28$ ). Each color and symbol represent individual species. All datasets are fitted with a power-law regression line. A positive correlation of nucleus volume over genomic content is only detected in interspecies datasets for certain selected cell types, such as female gametes (B) and erythrocytes (C) from multicellular eukaryotes, but not when using interspecies datasets from all measured cell types (A). All datasets in this figure and the individual measurements are available in Tables S1 and S2, respectively.

eukaryotes. Using these representative cells, I plotted the nuclear volume against genomic content (Fig. 2B). Even so, the coefficient of determination was still weak in prokaryotes ( $P=0.717, R^2=0.003$ )

and unicellular eukaryotes ( $P=0.439, R^2=0.029$ ), although it increased in oocytes ( $P<0.001, R^2=0.313$ ), suggesting a positive correlation with the genomic content in multicellular eukaryotes ( $A'=1.223\pm 0.283$ ). This positive correlation was also detected in non-dividing nucleated erythrocytes in metazoan species ( $A'=1.049\pm 0.110$ ;  $P<0.001, R^2=0.770$ ; Fig. 2C) (Cavalier-Smith, 1982; Gregory, 2001; Mueller et al., 2008). The estimated hyperallometry ( $A'>1$ ) of scaling exponents is consistent with the data obtained from intraspecies comparison in human cells with different DNA ploidy, including megakaryocytes, cardiomyocyte and others ( $A'=1.85$ ; estimated from Gillooly et al., 2015). These interspecies comparisons using cells that had time to reach a nuclear volume plateau, suggest a correlation between nuclear volume and genomic content only in multicellular eukaryotes – not in unicellular eukaryotes and prokaryotes. It should be noticed that the genomic content also correlates with cell size (Fig. S2A) but not with the N/C volume ratio (Fig. S2B). This relationship between cell volume and genomic content confirms that genome content correlates with both cell size and nuclear size (Gillooly et al., 2015). From these correlations, I speculate that, across the tree of life, the size of the nucleus or nucleoid can be modulated by changing the genomic content; although, the cell volume, which generally correlates with DNA content, might mask the effects of genomic content in determining nuclear size. In fact, when the nuclear volumes within an individual species that exhibits different DNA ploidy – for instance, through polyploidization – are compared, a positive correlation of nuclear size with genomic content can be found in several prokaryotic and eukaryotic species, including humans (Gillooly et al., 2015), frogs (Jevtić and Levy, 2017; Heijo et al., 2019 preprint), plants (Robinson et al., 2018), yeasts (Neumann and Nurse, 2007; Jorgensen et al., 2007) and bacteria (Gray et al., 2019). Some studies that have used *X. laevis* embryos *in vivo* as well as egg extracts support a correlation between nuclear volume and genomic content when the DNA content is changed experimentally, while the same cytoplasmic volume is maintained (Levy and Heald, 2010; Heijo et al., 2019 preprint), or when the nuclear number is increased with constant cytoplasmic volume (Boudreau et al., 2018 preprint; Novokova et al., 2016). This evidence suggests that the genomic content negligibly contributes to the determination of the nuclear volume, regardless of the contributions of the cell volume in determining the nuclear volume. In summary, during evolution, organisms seem to have acquired distinct regimes to control the size of their nuclei or nucleoid. These might be based on cytoplasmic properties or changes of the chromatin structure, which could have resulted in either a visible contribution of the genomic content to nuclear-size scaling in multicellular eukaryotes or the superficial lack of such a contribution in unicellular organisms.

To gain more insight into the contribution genomic content has in determining nuclear size, I calculated the ratio of genomic content to nuclear volume (GC/NV ratio) – which is equivalent to the DNA density inside the nucleus – for each category (Fig. 3A). The calculated GC/NV ratio is not constant between different species, which could be because the correlation between genomic content and nuclear volume in each category is reduced (Fig. 2). Nevertheless, there is a substantial difference in the range of the GC/NV ratios among the different categories. In prokaryote nucleoids, the GC/NV ratio only varies approximately within one order of magnitude, i.e. from  $\sim 1$  to  $\sim 30$ , which is considerably less than the three orders of magnitudes, i.e. from  $\sim 1$  to  $\sim 1000$ , observed in unicellular eukaryotes (Fig. 3A, spreading at longitudinal axis). This implies that the presence of nuclear membranes in unicellular eukaryotes can constrain more of the available space for DNA, compared with

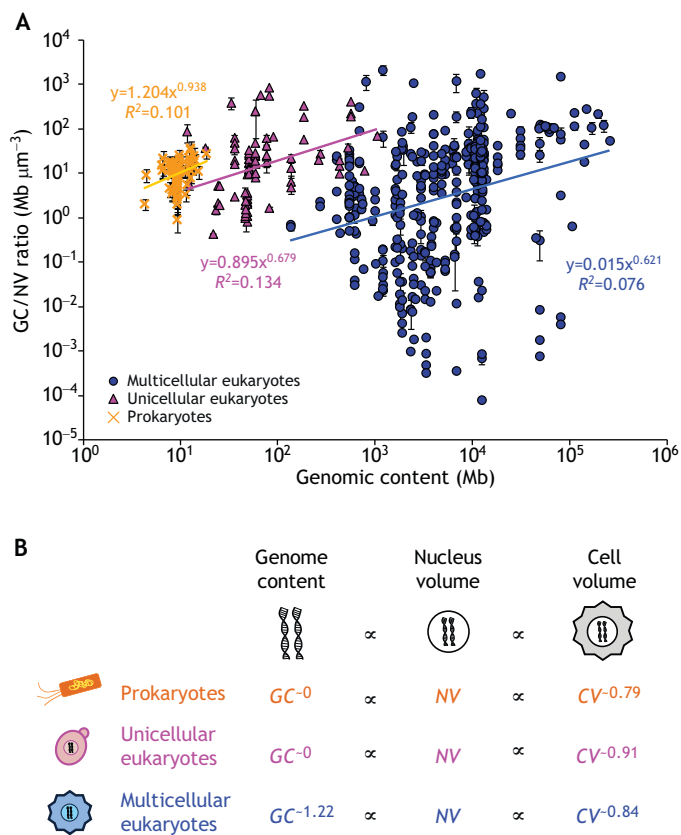


**Fig. 3. The ratio of genomic content to nuclear volume (GC/NV ratio) reveals tremendous variation, especially when comparing multicellular eukaryotes.** (A) DNA density in the nucleus or nucleoid, i.e. the ratio of genomic content to nuclear volume (GC/NV ratio), is plotted against the genomic content for various cell types, excluding during early embryonic development of multicellular organisms (multicellular eukaryotes:  $n=397$ ; unicellular eukaryotes:  $n=84$ ; prokaryotes:  $n=106$ ). Data are represented as the mean ( $\pm$ s.d.) of each sample and were fitted with a power-law regression line in each category. The equation and coefficient of determination ( $R^2$ ) are indicated. All datasets in this figure and individual measurement datasets are available in Tables S1 and S2, respectively. (B) Schematic summarizing the size scaling of nuclei and nucleoids across the tree of life. GC, genome content; NV, nuclear volume; CV, cell volume.

prokaryotes, which lack a nuclear membrane. Furthermore, in the nuclei of multicellular eukaryotes, where the chromatin interacts physically with nuclear membrane, the GC/NV ratio exhibited a tremendous variation of seven orders of magnitude (from  $\sim 0.0005$  to  $\sim 1000$ ). In higher eukaryotes, such as metazoans, a structure underneath the nuclear membrane, known as the nuclear lamina, enables interactions with chromatin (Mans et al., 2004; Ciska and Moreno Díaz de la Espina, 2014). This interaction between DNA and nuclear membrane, and mechanical stiffness of the lamina may help in transmitting the forces for the inward shrinking and outward expanding of chromatin to the nuclear membranes, to promote changes in nuclear size and in generating a nuclear rigidity to maintain either an extremely large or small nuclear size.

### Conclusions and perspectives

The inter-species comparison of nuclear size presented here indicates that the size-scaling properties of nuclei and nucleoids are quantitatively different among multicellular eukaryotes, unicellular eukaryotes and prokaryotes (Fig. 3B), although a general correlation of nuclear size with cell size is conserved across the tree of life. In fact,

prokaryotic nucleoids and eukaryotic nuclei show a hypoallometric scaling relationship with the cell volume. Such a hypoallometric relationship with the cell volume is also observed in the size scaling of mitotic spindles from diverse nematodes (scaling exponent  $A \sim 0.65$ ) (Farhadifar et al., 2015) and of chloroplasts from phototrophic eukaryotes ( $A \sim 0.83$ ) (Okie et al., 2016). Indeed, mitotic spindle length in most eukaryotes is known to be regulated by the dynamics of spindle microtubules and has a positive correlation with the cell size (Good et al., 2013; Hazel et al., 2013; Lacroix et al., 2018). When manipulating the number of aligned chromosomes at the metaphase plate in multicellular eukaryotes, which should correspond to the genomic content, the spindle length was altered by changing the alignment or dynamics of spindle microtubules (Hara and Kimura, 2013; Young et al., 2014; Dinarina et al., 2009). In prokaryotes, the chromatids can be partitioned into daughter cells without utilizing the spindle apparatus (Jun and Mudler, 2006), implying there is no scaling-relationship between genomic content and spindle length. The involvement of genomic content in controlling spindle length is expected to occur only in higher eukaryotes, and is evident for both the interphase nucleus and mitotic spindle. Accordingly, the mechanisms underlying size-scaling control may share common regulators between the nucleus and mitotic spindle, such as importin  $\alpha$  (Brownlee and Heald, 2019) and lamin (Tsai et al., 2006). As the ratio between DNA amount and interphase nuclear volume correlates with the size of condensed chromosomes within the mitotic spindle in multicellular eukaryotes (Hara et al., 2013, 2016; Ladouceur et al., 2015), the nuclear size scales with the sizes of other organelles, as well as the size of the spindle itself. Nonetheless, the scaling exponent of the size of other organelles with the cell volume is different; for instance, for mitochondria,  $A$  is  $\sim 1.06$  among eukaryotes (Okie et al., 2016) when compared to the hypoallometric scaling of the nucleus and mitotic spindle. A more-precise comparison of the scaling relationship between organelles across diverse species will be required to obtain a comprehensive view of the size-scaling properties inside the cell and the possible implications for evolutionary processes of intracellular structures.

From an evolutionary perspective, the observed qualitative correlation of nuclear volume with cell volume (Fig. 1A) implies that the basic concept of nuclear-size scaling with cell volume is common across eukaryotes. However, differences in the nuclear scaling exponent with cell volume (Fig. 1A) and a high variation in the GC/NV ratio (Fig. 3A) are also observed among the different categories of cellularity, which suggests that different mechanisms underlying the scaling with cell volume have been evolved. In addition to the known mechanisms through the supply of nuclear constituents from cytoplasm (Levy and Heald, 2010; Hara and Merten, 2015), I hypothesize that the size-scaling properties and their underlying mechanisms have been modulated by the differences in the molecular and structural constituents of the nuclear lamina and chromatin inside the nucleus across the tree of life. It is intuitive to consider that the size-scaling properties of the prokaryotic nucleoid can be attributed to the lack of a membrane around the genomic DNA and a topologically different circular chromosome. For eukaryotic nuclei, previous experimental studies have proposed that the amount of nuclear lamina constituents and lipid membranes is expected to be proportional to the cytoplasmic volume, and acts as determinants for nuclear size across eukaryotes (Levy and Heald, 2010; Hara and Merten, 2015). Although lipid membranes are common among eukaryotes, one remarkable difference is the existence of a nuclear lamina, typically composed of lamins, which is only present in multicellular eukaryotes. In fact, most unicellular organisms including fungi

and yeasts do not have lamin genes (Mans et al., 2004; Ciska and Moreno Díaz de la Espina, 2014). Lamins underneath the nuclear membrane can associate with chromatin and form structures called lamin-associated domains (van Steensel and Belmont, 2017). Together with the observed correlation between nuclear volume and genomic content, which is only found in multicellular eukaryotes (Fig. 2), I therefore propose that the ability of chromatin to interact with the nuclear membrane can transmit the physical properties of chromatin to the nuclear membrane (Fig. 4). Previous experimental studies have suggested that the chromatin inside the nucleus works as a viscoelastic spring to impact on nuclear stiffness and to determine nuclear size (Shimamoto et al., 2017; Stephens et al., 2017; Chan et al., 2017; Heijo et al., 2019 preprint). Upon manipulation of the physical chromatin structure – through altering the repulsion forces from negatively charged DNA or modifying the epigenetic status of chromatin, while maintaining nuclear lamina – the resulting nuclear stiffness and nuclear size are changed in mammalian cell cultures *in vivo*, in isolated nuclei or in *X. laevis* egg extracts (Shimamoto et al., 2017; Stephens et al., 2017; Chan et al., 2017; Heijo et al., 2019 preprint). Under this assumption – if chromatin was highly condensed – DNA-exerted repulsion forces, which correspond to the strength of the chromatin spring would be small, resulting in decreased expansion forces of the nuclear membrane from inside (Fig. 4). As epigenetic modifications of chromatin are considered to be much more

complex in metazoans as compared to unicellular eukaryotes (Hinman and Cary, 2017; Tang et al., 2012), the epigenetically modified chromatin of multicellular eukaryotes might result in either a more-condensed and stiffer or a more-decondensed and softer conformation. This could then change the nuclear volume and DNA density inside the nucleus, consistent with the observation of tremendous variation of GC/NV ratios in multicellular eukaryotes only (Fig. 3). In addition, the lamina structure itself has a mechanical stiffness, generating rigidity to counteract against the changes in forces due to the chromatin spring and maintaining the nuclear size (Stephens et al., 2017). This stiffness is determined by the ratio of A-type lamin to B-type lamin in metazoans (Swift et al., 2013), as well as by the occasional incorporation of cytoskeletal actin fibers into the nucleus in amphibian oocytes and early embryos (Feric and Brangwynne, 2013; Oda et al., 2017). The nuclear actin fibers stabilize intranuclear components when the nuclear volume becomes sufficiently large to be affected by the gravitational force (Feric and Brangwynne, 2013). Therefore, the mechanical stiffness of the nuclear lamina is expected to help the nucleus to maintain a certain nuclear size, regardless of the physical chromatin structures. Since the nuclear lamina contributes to these counteracting functions, i.e. the transmission forces from the chromatin and nuclear stiffness (Shimamoto et al., 2017; Stephens et al., 2019), balancing these would allow the nucleus in multicellular eukaryotes to generate tremendous variation of DNA density. Nevertheless, it

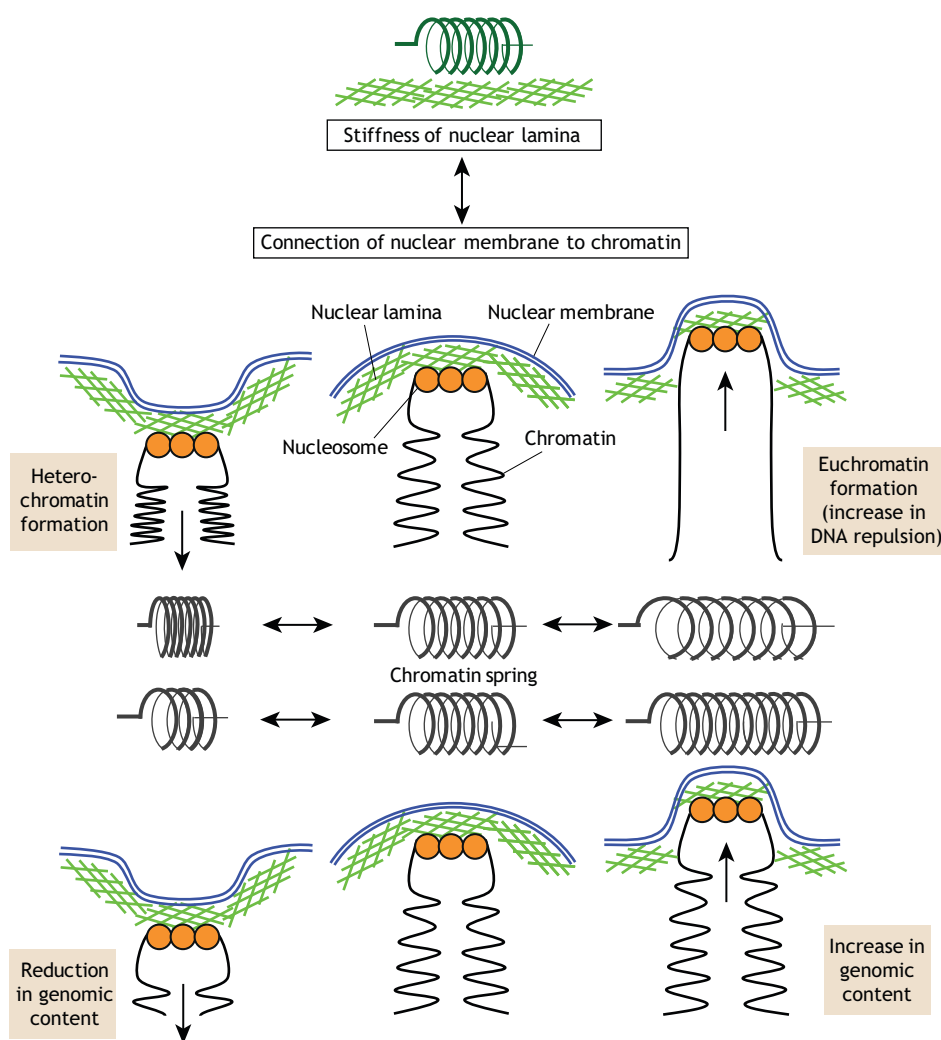


**Fig. 4. Overview of the putative functions of nuclear lamina in higher eukaryotes.** The lamina underneath the nuclear membrane, which is generally organized by lamins, has a mechanical stiffness to prevent the deformation of the nuclear membrane (top) and serves as a mechanical transmitter of forces from chromatin inside the nucleus (bottom). The chromatin conformation generates forces to pull or push on the nuclear membrane caused by the physical state of chromatin. When the chromatin organizes heterochromatin or the genome content is reduced, the nuclear membrane that is connected with chromatin is pulled inwards (left), resulting in a small increase in nuclear size. When the chromatin organizes euchromatin (and/or increases the repulsion force) or the genome content increases, the nuclear membrane linked to chromatin is pushed outwards (right), resulting in a large increase in nuclear size.

should be noticed that the lamina structure is not thick enough to generate the same rigidity as the actin and microtubule cytoskeletons (Turgay et al., 2017), suggesting the structural function of nuclear lamina on nuclear stiffness is smaller than expected.

What is the biological significance of this tremendous variation of DNA density in higher eukaryotes? Lesser DNA density might create more space in the nucleoplasm and promote the subcompartmentalization of membrane-less organelles, such as nucleolus, Cajal body, P body, nuclear speckles and others. By contrast, crowding under conditions of high DNA density inside the nucleus might promote subcompartmentalization through liquid-liquid phase transitions, resulting in formation of a nucleolus and heterochromatin (Weber and Brangwynne, 2015; Strom et al., 2017). Although it is unclear whether changes in nuclear size-scaling properties can, indeed, drive the evolution of intranuclear functions, the specific features of higher-eukaryotes with regard to nuclear size and DNA density have the potential to modulate intranuclear properties and functions. Future experimental and theoretical studies to evaluate the effects size and density of the nucleus have, and to precisely compare the nuclear size-scaling relationship between and within species, will help to shed light on the evolution of the eukaryotic nucleus.

#### Acknowledgements

I thank members of my laboratory and the Center for Promotion of Integrated Sciences (CPIS) of SOKENDAI, the Research Organization of Information and Systems (ROIS) (Sokendai, Japan) for helping with the data collection, as well as Kazunori Kume for discussions regarding the manuscript.

#### Competing interests

The author declares no competing or financial interests.

#### Funding

This work is supported by the Home for Innovative Researchers and Academic Knowledge Users (HIRAKU) consortium and a Grant-in-Aid for Challenging Exploratory Research from Japan Society for the Promotion of Science (16K14727).

#### Supplementary information

Supplementary information available online at  
<http://jcs.biologists.org/lookup/doi/10.1242/jcs.241869.supplemental>

#### References

- Anderson, D. J. and Hetzer, M. W.** (2007). Nuclear envelope formation by chromatin-mediated reorganization of the endoplasmic reticulum. *Nat. Cell Biol.* **9**, 1160–1166. doi:10.1038/ncb1636
- Arata, Y., Takagi, H., Sako, Y. and Sawa, H.** (2015). Power law relationship between cell cycle duration and cell volume in the early embryonic development of *Caenorhabditis elegans*. *Front. Physiol.* **5**, 529. doi:10.3389/fphys.2014.00529
- Boveri, T.** (1905). Zellenstudien V. Über die Abhängigkeit der Kerngröße und Zellenzahl der Seeigel-Larven von der Chromosomenzahl der Ausgangszellen. *Jenaische Z. Naturw.* **39**, 445–524.
- Boudreau, V., Hazel, J., Sellinger, J., Chen, P., Manakova, K., Radzynski, R., Garcia, H., Allard, J., Gatlin, J. and Maddox, P.** (2018). Nucleo-cytoplasmic trafficking regulates nuclear surface area during nuclear organogenesis. *bioRxiv*, 326140. doi:10.1101/326140
- Brownlee, C. and Heald, R.** (2019). Importin  $\alpha$  partitioning to the plasma membrane regulates intracellular scaling. *Cell* **176**, 805–815.e8. doi:10.1016/j.cell.2018.12.001
- Cantwell, H. and Nurse, P.** (2019a). A systematic genetic screen identifies essential factors involved in nuclear size control. *PLoS Genet.* **15**, e1007929. doi:10.1371/journal.pgen.1007929
- Cantwell, H. and Nurse, P.** (2019b). Unravelling nuclear size control. *Curr. Genet.* **65**, 1281–1285. doi:10.1007/s00294-019-00999-3
- Cavalier-Smith, T.** (1982). Skeletal DNA and the evolution of genome size. *Annu. Rev. Biophys. Bioeng.* **11**, 273–302. doi:10.1146/annurev.bb.11.060182.001421
- Cavalier-Smith, T.** (1985). Cell volume and the evolution of genome size. In *The Evolution of Genome Size* (ed. T. Cavalier-Smith), pp. 105–184. Chichester: Wiley.
- Chan, C. J., Li, W., Cojoc, G. and Guck, J.** (2017). Volume transitions of isolated cell nuclei induced by rapid temperature increase. *Biophys. J.* **112**, 1063–1076. doi:10.1016/j.bpj.2017.01.022
- Chang, A. Y. and Marshall, W. F.** (2017). Organelles – understanding noise and heterogeneity in cell biology at an intermediate scale. *J. Cell Sci.* **130**, 819–826. doi:10.1242/jcs.181024
- Ciska, M. and Moreno Díaz de la Espina, S.** (2014). The intriguing plant nuclear lamina. *Front. Plant Sci.* **5**, 166. doi:10.3389/fpls.2014.00166
- Conklin, E. G.** (1912). Cell size and nuclear size. *J. Exp. Zool.* **12**, 1–98. doi:10.1002/jez.1400120102
- Dinarina, A., Pugieux, C., Corral, M. M., Loose, M., Spatz, J., Karsenti, E. and Nédélec, F.** (2009). Chromatin shapes the mitotic spindle. *Cell* **138**, 502–513. doi:10.1016/j.cell.2009.05.027
- Edens, L. J., White, K. H., Jevtic, P., Li, X. and Levy, D. L.** (2013). Nuclear size regulation: from single cells to development and disease. *Trends Cell Biol.* **23**, 151–159. doi:10.1016/j.tcb.2012.11.004
- Edens, L. J., Dilksaver, M. R. and Levy, D. L.** (2017). PKC-mediated phosphorylation of nuclear lamins at a single serine residue regulates interphase nuclear size in *Xenopus* and mammalian cells. *Mol. Biol. Cell* **28**, 1389–1399. doi:10.1091/mbc.e16-11-0786
- Fankhauser, G.** (1945). Maintenance of normal structure in heteroploid salamander larvae, through compensation of changes in cell size by adjustment of cell number and cell shape. *J. Exp. Zool.* **100**, 445–455. doi:10.1002/jez.1401000310
- Farhadifar, R., Baer, C. F., Valfort, A.-C., Andersen, E. C., Müller-Reichert, T., Delattre, M. and Needleman, D. J.** (2015). Scaling, selection, and evolutionary dynamics of the mitotic spindle. *Curr. Biol.* **25**, 732–740. doi:10.1016/j.cub.2014.12.060
- Feric, M. and Brangwynne, C. P.** (2013). A nuclear F-actin scaffold stabilizes ribonucleoprotein droplets against gravity in large cells. *Nat. Cell Biol.* **15**, 1253–1259. doi:10.1038/ncb2830
- Gillooly, J. F., Hein, A. and Damiani, R.** (2015). Nuclear DNA content varies with cell size across human cell types. *Cold Spring Harb. Perspect. Biol.* **7**, a019091. doi:10.1101/cshperspect.a019091
- Goehring, N. W. and Hyman, A. A.** (2012). Organelle growth control through limiting pools of cytoplasmic components. *Curr. Biol.* **22**, R330–R339. doi:10.1016/j.cub.2012.03.046
- Good, M. C., Vahey, M. D., Skandarajah, A., Fletcher, D. A. and Heald, R.** (2013). Cytoplasmic volume modulates spindle size during embryogenesis. *Science* **342**, 856–860. doi:10.1126/science.1243147
- Gray, W. T., Govers, S. K., Xiang, Y., Parry, B. R., Campos, M., Kim, S. and Jacobs-Wagner, C.** (2019). Nucleo-cell size scaling and intracellular organization of translation across bacteria. *Cell* **177**, 1632–1648.e20. doi:10.1016/j.cell.2019.05.017
- Gregory, T. R.** (2001). The bigger the C-Value, the larger the cell: genome size and red blood cell size in vertebrates. *Blood Cells Mol. Dis.* **27**, 830–843. doi:10.1006/bcmd.2001.0457
- Hara, Y. and Kimura, A.** (2011). Cell-size-dependent control of organelle sizes during development. In "Cell Cycle in Development", Vol. 53: Series –Results and Problems in Cell Differentiation (ed. J. Z. Kubiak), pp. 93–108. Springer.
- Hara, Y. and Kimura, A.** (2013). An allometric relationship between mitotic spindle width, spindle length, and ploidy in *Caenorhabditis elegans* embryos. *Mol. Biol. Cell* **24**, 1411–1419. doi:10.1091/mbc.e12-07-0528
- Hara, Y. and Merten, C. A.** (2015). Dynein-based accumulation of membranes regulates nuclear expansion in *Xenopus laevis* egg extracts. *Dev. Cell* **33**, 562–575. doi:10.1016/j.devcel.2015.04.016
- Hara, Y., Iwabuchi, M., Ohsumi, K. and Kimura, A.** (2013). Intracellular DNA density affects chromosome condensation in metazoans. *Mol. Biol. Cell* **24**, 2442–2453. doi:10.1091/mbc.e13-01-0043
- Hara, Y., Adachi, K., Kagohashi, S., Yamagata, K., Tanabe, H., Kikuchi, S., Okumura, S. I. and Kimura, A.** (2016). Scaling relationship between intra-nuclear DNA density and chromosomal condensation in metazoan and plant. *Chromosome Sci.* **19**, 43–49.
- Hazel, J., Krutkramelis, K., Mooney, P., Tomschik, M., Gerow, K., Oakey, J. and Gatlin, J. C.** (2013). Changes in cytoplasmic volume are sufficient to drive spindle scaling. *Science* **342**, 853–856. doi:10.1126/science.1243110
- Heijo, H., Shimogama, S., Nakano, S., Miyata, A., Iwao, Y. and Hara, Y.** (2019). DNA content contributes to nuclear size control in *Xenopus*. *Sneak Peek* **2**, 64. doi:10.2139/ssrn.3461734
- Hertwig, R.** (1903). Ueber die korrelation von zell-und kerngrösse und ihre bedeutung für die geschlechtliche differenzierung und die teilung der zelle. *Biol. Centralbl.* **23**, 49–62.
- Hinman, V. and Cary, G.** (2017). The evolution of gene regulation. *eLife* **6**, e27291. doi:10.7554/elife.27291
- Jevtić, P. and Levy, D. L.** (2015). Nuclear size scaling during *Xenopus* early development contributes to midblastula transition timing. *Curr. Biol.* **25**, 45–52. doi:10.1016/j.cub.2014.10.051
- Jevtić, P. and Levy, D. L.** (2017). Both nuclear size and DNA amount contribute to midblastula transition timing in *Xenopus laevis*. *Sci. Rep.* **7**, 7908. doi:10.1038/s41598-017-08243-z
- Jevtić, P., Edens, L. J., Li, X., Nguyen, T., Chen, P. and Levy, D. L.** (2015). Concentration-dependent effects of nuclear lamins on nuclear size in *Xenopus* and mammalian cells. *J. Biol. Chem.* **290**, 27557–27571. doi:10.1074/jbc.M115.673798

- Jorgensen, P., Edgington, N. P., Schneider, B. L., Rupeš, I., Tyers, M. and Futcher, B. (2007). The size of the nucleus increases as yeast cells grow. *Mol. Biol. Cell* **18**, 3523–3532. doi:10.1091/mbc.e06-10-0973
- Jun, S. and Mulder, B. (2006). Entropy-driven spatial organization of highly confined polymers: lessons for the bacterial chromosome. *Proc. Natl. Acad. Sci. USA* **103**, 12388–12393. doi:10.1073/pnas.0605305103
- Kume, K., Cantwell, H., Neumann, F. R., Jones, A. W., Snijders, A. P. and Nurse, P. (2017). A systematic genomic screen implicates nucleocytoplasmic transport and membrane growth in nuclear size control. *PLoS Genet.* **13**, e1006767. doi:10.1371/journal.pgen.1006767
- Kume, K., Cantwell, H., Burrell, A. and Nurse, P. (2019). Nuclear membrane protein Lem2 regulates nuclear size through membrane flow. *Nat. Commun.* **10**, 1871. doi:10.1038/s41467-019-109623-x
- Lacroix, B., Letort, G., Pitayu, L., Sallé, J., Stefanutti, M., Maton, G., Ladouceur, A.-M., Canman, J. C., Maddox, P. S., Maddox, A. S. et al. (2018). Microtubule dynamics scale with cell size to set spindle length and assembly timing. *Dev. Cell* **45**, 496–511.e6. doi:10.1016/j.devcel.2018.04.022
- Ladouceur, A.-M., Dorn, J. F. and Maddox, P. S. (2015). Mitotic chromosome length scales in response to both cell and nuclear size. *J. Cell Biol.* **209**, 645–651. doi:10.1083/jcb.201502092
- Levy, D. L. and Heald, R. (2010). Nuclear size is regulated by importin  $\alpha$  and Ntf2 in *Xenopus*. *Cell* **143**, 288–298. doi:10.1016/j.cell.2010.09.012
- Levy, D. L. and Heald, R. (2012). Mechanisms of intracellular scaling. *Annu. Rev. Cell Dev. Biol.* **28**, 113–135. doi:10.1146/annurev-cellbio-092910-154158
- Maeshima, K., Iino, H., Hihara, S., Funakoshi, T., Watanabe, A., Nishimura, M., Nakatomi, R., Yahata, K., Imamoto, F., Hashikawa, T. et al. (2010). Nuclear pore formation but not nuclear growth is governed by cyclin-dependent kinases (Cdks) during interphase. *Nat. Struct. Mol. Biol.* **17**, 1065–1071. doi:10.1038/nsmb.1878
- Mans, B. J., Anantharaman, V., Aravind, L. and Koonin, E. V. (2004). Comparative genomics, evolution and origins of the nuclear envelope and nuclear pore complex. *Cell Cycle* **3**, 1612–1637. doi:10.4161/cc.3.12.1316
- Marshall, W. F. (2015). Subcellular size. *Cold Spring Harb. Perspect. Biol.* **7**, a019059. doi:10.1101/cshperspect.a019059
- Milo, R. and Philips, R. (2016). Size and geometry. In *Cell Biology by the Numbers*, pp. 3–63. New York, NY: Garland Science.
- Mueller, R. L., Gregory, T. R., Gregory, S. M., Hsieh, A. and Boore, J. L. (2008). Genome size, cell size, and the evolution of enucleated erythrocytes in attenuate salamanders. *Zoology (Jena)* **111**, 218–230. doi:10.1016/j.zool.2007.07.010
- Neumann, F. R. and Nurse, P. (2007). Nuclear size control in fission yeast. *J. Cell Biol.* **179**, 593–600. doi:10.1083/jcb.200708054
- Neurohr, G., Naegeli, A., Titos, I., Theler, D., Greber, B., Díez, J., Gabaldón, T., Mendoza, M. and Barral, Y. (2011). A midzone-based ruler adjusts chromosome compaction to anaphase spindle length. *Science* **332**, 465–468. doi:10.1126/science.1201578
- Novakova, L., Kovacovicova, K., Dang-Nguyen, T. Q., Sodek, M., Skultety, M. and Anger, M. (2016). A balance between nuclear and cytoplasmic volumes controls spindle length. *PLoS ONE* **11**, e0149535. doi:10.1371/journal.pone.0149535
- Oda, H., Shirai, N., Ura, N., Ohsumi, K. and Iwabuchi, M. (2017). Chromatin tethering to the nuclear envelope by nuclear actin filaments: a novel role of the actin cytoskeleton in the *Xenopus* blastula. *Genes Cells* **22**, 376–391. doi:10.1111/gtc.12483
- Okie, J. G., Smith, V. H. and Martin-Cereceda, M. (2016). Major evolutionary transitions of life, metabolic scaling and the number and size of mitochondria and chloroplasts. *Proc. R. Soc. B* **283**, 20160611. doi:10.1098/rspb.2016.0611
- Price, H. J., Sparrow, A. H. and Nauman, A. F. (1973). Correlations between nuclear volume, cell volume and DNA content in meristematic cells of herbaceous angiosperms. *Experientia* **29**, 1028–1029. doi:10.1007/BF01930444
- Robinson, D. O., Coate, J. E., Singh, A., Hong, L., Bush, M., Doyle, J. J. and Roeder, A. H. K. (2018). Ploidy and size at multiple scales in the *Arabidopsis* Sepal. *Plant Cell* **30**, 2308–2329. doi:10.1105/tpc.18.00344
- Schubert, I. and Oud, J. L. (1997). There is an upper limit of chromosome size for normal development of an organism. *Cell* **88**, 515–520. doi:10.1016/S0092-8674(00)81891-7
- Shimamoto, Y., Tamura, S., Masumoto, H. and Maeshima, K. (2017). Nucleosome-nucleosome interactions via histone tails and linker DNA regulate nuclear rigidity. *Mol. Biol. Cell* **28**, 1580–1589. doi:10.1091/mbc.e16-11-0783
- Šimová, I. and Herben, T. (2012). Geometrical constraints in the scaling relationships between genome size, cell size and cell cycle length in herbaceous plants. *Proc. R. Soc. B* **279**, 867–875. doi:10.1098/rspb.2011.1284
- Stephens, A. D., Banigan, E. J., Adam, S. A., Goldman, R. D. and Marko, J. F. (2017). Chromatin and lamin A determine two different mechanical response regimes of the cell nucleus. *Mol. Biol. Cell* **28**, 1984–1996. doi:10.1091/mbc.e16-09-0653
- Stephens, A. D., Banigan, E. J. and Marko, J. F. (2019). Chromatin's physical properties shape the nucleus and its functions. *Curr. Opin. Cell Biol.* **58**, 76–84. doi:10.1016/j.ceb.2019.02.006
- Strom, A. R., Emelyanov, A. V., Mir, M., Fyodorov, D. V., Darzacq, X. and Karpen, G. H. (2017). Phase separation drives heterochromatin domain formation. *Nature* **547**, 241–245. doi:10.1038/nature22989
- Swift, J., Ivanovska, I. L., Buxboim, A., Harada, T., Dingal, P. C. D. P., Pinter, J., Pajerowski, J. D., Spinler, K. R., Shin, J.-W., Tewari, M. et al. (2013). Nuclear lamin-A scales with tissue stiffness and enhances matrix-directed differentiation. *Science* **341**, 1240104. doi:10.1126/science.1240104
- Tang, Y., Gao, X.-D., Wang, Y., Yuan, B.-F. and Feng, Y.-Q. (2012). Widespread existence of cytosine methylation in yeast DNA measured by gas chromatography/mass spectrometry. *Anal. Chem.* **84**, 7249–7255. doi:10.1021/ac301727c
- Tsai, M.-Y., Wang, S., Heidinger, J. M., Shumaker, D. K., Adam, S. A., Goldman, R. D. and Zheng, Y. (2006). A mitotic lamin B matrix induced by RanGTP required for spindle assembly. *Science* **311**, 1887–1893. doi:10.1126/science.1122771
- Tschlaki, E. and FitzHarris, G. (2016). Nucleus downscaling in mouse embryos is regulated by cooperative developmental and geometric programs. *Sci. Rep.* **6**, 28040. doi:10.1038/srep28040
- Turgay, Y., Eibauer, M., Goldman, A. E., Shimi, T., Khayat, M., Ben-Harush, K., Dubrovsky-Gaupp, A., Sapra, K. T., Goldman, R. D. and Medalia, O. (2017). The molecular architecture of lamins in somatic cells. *Nature* **543**, 261–264. doi:10.1038/nature21382
- Ulbert, S., Platani, M., Boue, S. and Mattaj, I. W. (2006). Direct membrane protein-DNA interactions required early in nuclear envelope assembly. *J. Cell Biol.* **173**, 469–476. doi:10.1083/jcb.200512078
- Uppaluri, S., Weber, S. C. and Brangwynne, C. P. (2016). Hierarchical size scaling during multicellular growth and development. *Cell Rep.* **17**, 345–352. doi:10.1016/j.celrep.2016.09.007
- van Steensel, B. and Belmont, A. S. (2017). Lamina-associated domains: links with chromosome architecture, heterochromatin, and gene repression. *Cell* **169**, 780–791. doi:10.1016/j.cell.2017.04.022
- Vinogradov, A. E. and Anatskaya, O. V. (2006). Genome size and metabolic intensity in tetrapods: a tale of two lines. *Proc. R. Soc. B* **273**, 27–32. doi:10.1098/rspb.2005.3266
- Walters, A. D., Amoateng, K., Wang, R., Chen, J.-H., McDermott, G., Larabell, C. A., Gadali, O. and Cohen-Fix, O. (2019). Nuclear envelope expansion in budding yeast is independent of cell growth and does not determine nuclear volume. *Mol. Biol. Cell* **30**, 131–145. doi:10.1091/mbc.E18-04-0204
- Weber, S. C. and Brangwynne, C. P. (2015). Inverse size scaling of the nucleolus by a concentration-dependent phase transition. *Curr. Biol.* **25**, 641–646. doi:10.1016/j.cub.2015.01.012
- Wesley, C. C., Mishra, S. and Levy, D. L. (2020). Organelle size scaling over embryonic development. *Wiley Interdiscip. Rev. Dev. Biol.*, e375. doi:10.1002/wdev.376
- Yamaguchi, M., Mori, Y., Kozuka, Y., Okada, H., Uematsu, K., Tame, A., Furukawa, H., Maruyama, T., Worman, C. O. D. and Yokoyama, K. (2012). Prokaryote or eukaryote? A unique microorganism from the deep sea. *J. Electron Microsc. (Tokyo)* **61**, 423–431. doi:10.1093/jmicro/dfs062
- Young, S., Besson, S. and Welburn, J. P. I. (2014). Length-dependent anisotropic scaling of spindle shape. *Biol. Open* **3**, 1217–1223. doi:10.1242/bio.201410363
- Zierhut, C., Jenness, C., Kimura, H. and Funabiki, H. (2014). Nucleosomal regulation of chromatin composition and nuclear assembly revealed by histone depletion. *Nat. Struct. Mol. Biol.* **21**, 617–625. doi:10.1038/nsmb.2845

## Materials and methods

### Data collection from published data

I explored the literature reporting absolute values of cell and nuclear volumes and visualizing the nucleus and/or whole cell using Google Scholar, Google Image and PubMed. When the cell or nuclear volumes were reported only on a graph, I estimated approximately values from the graph by measuring relative position of target data against the scales on the graph. When values in the cell or nuclear volume were not reported, I measured the major and minor axes of the nucleus or cell by using ImageJ from microscopic images and estimated the absolute length ( $L$ ) and width ( $W$ ) information based on the listed scale bar. I utilized the images, which could be detected for nucleus and/or whole cell visualized by staining using specific dyes or antibodies against DNA, nuclear membrane, nucleoplasmic proteins or cytoplasmic proteins, live-imaging with fluorescent-fused proteins or electron microscopic imaging. For simplifying the volume estimation, I excluded cells with complicated shape (non-spherical) such as adhesive culture cells due to inaccurate prediction and difficulty in estimating the height. To estimate the nuclear volume ( $NV$ ), I calculated the volume as  $NV = L/2 \times (W/2)^2 \times PI \times 4/3$  by assuming an oval sphere. In case of multiple nuclei inside the cell such as two pronuclei in the metazoan one-cell stage embryos, I used the total nuclear volume. To estimate the cell volume ( $CV$ ), I used different equations for the predicted 3-dimentional cell shape as  $CV = L/2 \times (W/2)^2 \times PI \times 4/3$  or  $(L/2)^2 \times W/2 \times PI \times 4/3$  for oval-sphere-shaped cells (e.g. *Caenorhabditis elegans* embryos),  $CV = (W/2)^2 \times PI \times L$  for cylindrical cells (e.g. fission yeast),  $CV = L^2 \times W$  or  $L \times W^2$  for cuboid cells (e.g. plant root tip cells surrounding rigid cell wall). After estimating the multiple data of nuclear, and cell volumes from the individual literatures, the averaged values were used for analyses and averaged values with standard deviation were shown in graphs. All data used in this study are listed in the electric supplementary material (Tables S1 and S2). The data were divided into three or four categories as multicellular eukaryotes (subdivided with heterotrophic and phototrophic organisms in some cases), unicellular eukaryotes and prokaryotes (including one archaea bacterium). The genome content is assumed as situations after DNA replication and 4N (4-fold of genome size) in eukaryotes and 2N in prokaryotes if the cell cycle information is unavailable. When the cell cycle is described as before S phase (like G1 phase), I assume the

reduced genome content as 2N in eukaryotes. When the genome size in the species remains unanalyzed, the genome content is estimated from the C-values.

## Data analysis

For showing graph of scaling relationship, all or categorized data were plotted and fitted with a power-law regression line using Excel software (Microsoft). For understanding the strength of correlation, the coefficient of determination ( $R^2$ ) was calculated using Excel software. The calculation of standard deviations (S.D.) and statistical difference against scaling exponent were done by regression analysis tool with two-sided Student's *t* test in Excel software using the  $\log_{10}$  transformed datasets.

For comparing the correlation with genomic content and exclude spontaneous variation in cell size regardless genome content, I used a single data point in each species as only female gamete, oocyte, in multicellular eukaryotes and data under more normal growth condition without any perturbation of genes in unicellular organisms.

## Supplemental figures

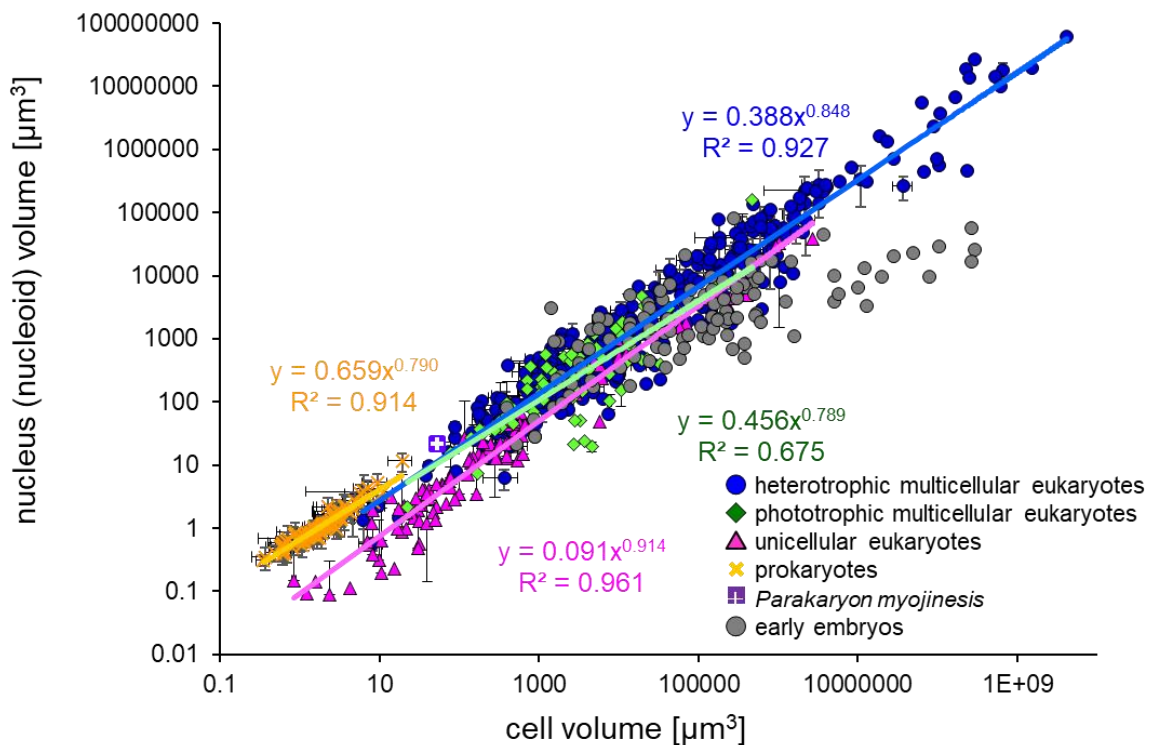


**Fig. S1: Size scaling of nucleus volume with cell volume.** (A) Size scaling of nucleus volume with cell volume in all data of various cell types. Data of heterotrophic multicellular eukaryotes (blue circles), phototrophic multicellular eukaryotes (green diamonds), unicellular eukaryotes (pink triangles), prokaryotes (orange crosses), and *Parakaryon myoijinesis* (purple cross) are identical to Fig. 1. Data from early embryos in multicellular eukaryotes are represented as grey circles.

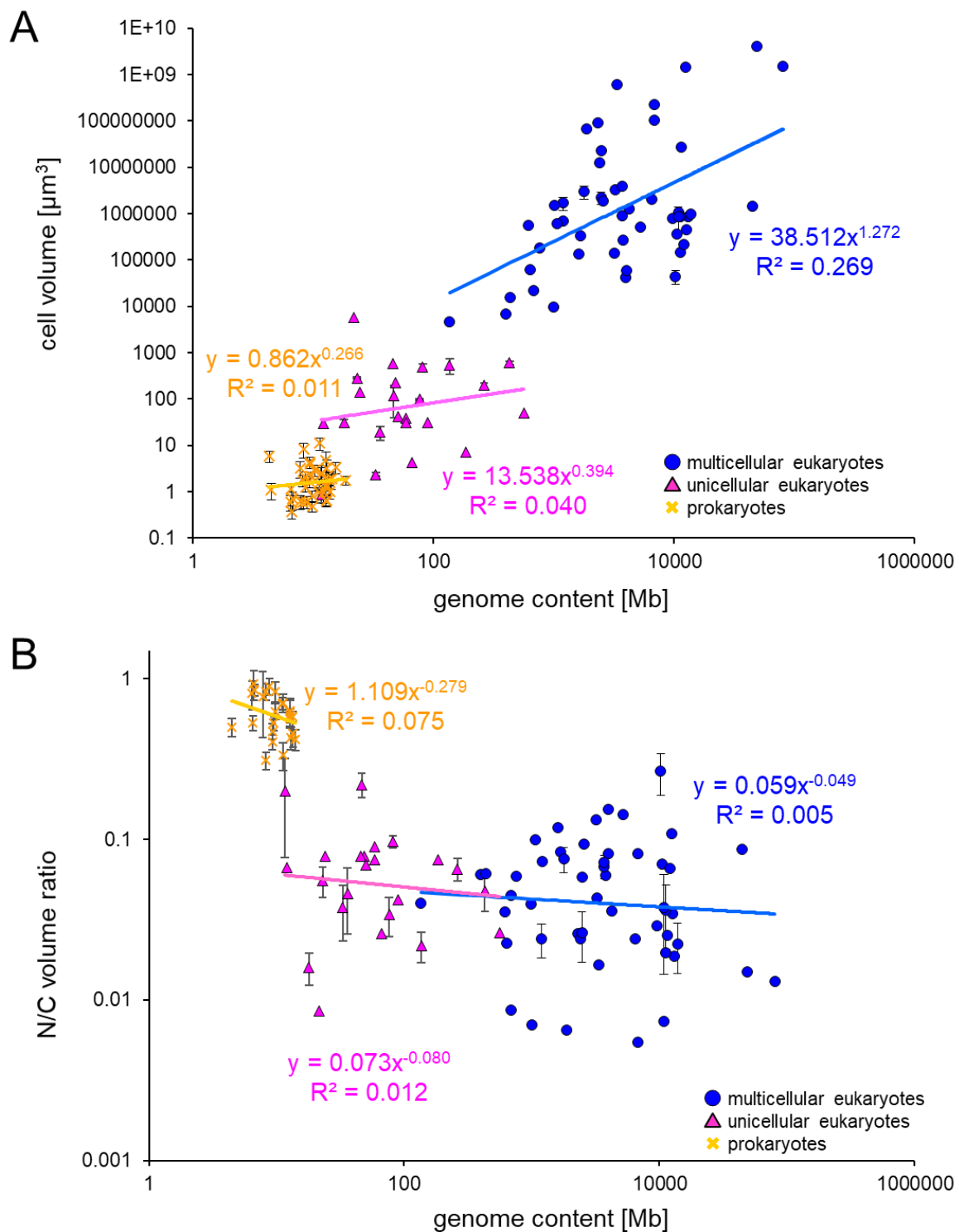


**Fig. S2: Scaling relationships with genome content.** (A) Size scaling of cell volume with genomic contents in data only including female gamete, which is fully grown oocyte, in multicellular organisms (blue;  $N = 50$ ) and wild type cells with normal growth condition in unicellular organisms (eukaryotes: pink,  $N = 23$ ; prokaryotes: orange,  $N = 40$ ). (B) Size scaling of N/C volume ratio with genomic contents in data only including female gamete in

multicellular eukaryotes and cells under normal growth condition in unicellular organisms. Each species with each DNA ploidy represents one symbol with error bar (S.D.). Data in each category are fitted with a power-law regression line.

## Supplemental tables

### Table S1. Mean values of GC, CV, NV, N/C volume ratio, and GC/NV ratio

Mean value, standard deviation (S.D.), and sample number (N) of parameters in each condition or cell type were shown. Phylum, species name, cell type (and/or growth condition), and references of images for measurements or numerical data was also shown. The procedures of measurement were categorized as A: genome size listed in literature; B: genome size predicted from C-value, no data: could not find any data for genome size; C: volume calculated as an oval ( $V = L/2 \times (W/2)^2 \times PI \times 4/3$  or  $= (L/2)^2 \times (W/2) \times PI \times 4/3$ ); D: volume calculated as a cylindrical shape ( $V = (W/2)^2 \times PI \times L$ ); E: volume calculated as a cuboid ( $CV = L^2 \times W$  or  $CV = L \times W^2$ ); F: value listed in the literature; G: value calculated from the listed parameter in the literature or estimated from the graph; H: value calculated from our estimated value; ND: no data. Light blue, orange, and green colours in tables represent data from early embryonic development in multicellular eukaryotes (excluded from Figs. 1–3), female gametes (fully-grown oocytes) of multicellular eukaryotes and unicellular organisms under normal growth condition (for Fig. 2B), and erythrocytes (for Fig. 2C), respectively.

[Click here to Download Table S1](#)

### Table S2. All collected data of CV, NV, N/C volume ratio, and GC/NV ratio in each condition

All measured or collected values for parameters were shown in each growth condition or cell type. NV/CV-R and GC/NV-R represent N/C volume ratio and GC/NV ratio, respectively.

[Click here to Download Table S2](#)

## Supplemental references

- Abbadie, C., Boucher, D., Charlemagne, J., Lacroix, J. C.** (1987). Immunolocalization of three oocyte nuclear proteins during oogenesis and embryogenesis in Pleurodeles. *Development*. **101**, 715–728
- Adonina, L. S., Podgornaya, O. I., Shaposhnikova, T. G.** (2012). Morphodynamics of the Contract Plate in the Course of Oocyte Maturation in the Scyphozoan Aurelia aurita (*Cnidaria: Semaeostomae*). *Russian J. Dev. Biol.* **43**(1), 17-24.
- Agerholm, I. E., Hnida, C., Crüger, D. G., Berg, C., Bruun-Petersen, G., Kølvraa, S., Ziebe, S.** (2008). Nuclei size in relation to nuclear status and aneuploidy rate for 13 chromosomes in donated four cells embryos. *J. Assist. Reprod. Genet.* **25**(2-3), 95-102.
- Akada, J. K. et al.** (2010). Helicobacter pylori CagA inhibits endocytosis of cytotoxin VacA in host cells. *Dis. Model. Mech.* **3**(9-10), 605-17.
- Ali, E. I., Loidl, J., Howard-Till, R. A.** (2018). A streamlined cohesin apparatus is sufficient for mitosis and meiosis in the protist Tetrahymena. *Chromosoma* **127**(4), 421-435.
- Amiel, A., Houliston, E.** (2009). Three distinct RNA localization mechanisms contribute to oocyte polarity establishment in the cnidarian *Clytia hemisphaerica*. *Dev. Biol.* **327**(1), 191-203.
- Apperson, K. D., Bird, K. E., Cherian, G., Löhr, C. V.** (2017). Histology of the Ovary of the Laying Hen (*Gallus domesticus*). *Vet. Sci.* **4**(4), E66.
- Azimzadeh, J., Nacry, P., Christodoulidou, A., Drevensek, S., Camilleri, C., Amiour, N., Parcy, F., Pastuglia, M., Bouchez, D.** (2008). Arabidopsis TONNEAU1 proteins are essential for preprophase band formation and interact with centrin. *Plant Cell* **20**(8), 2146-59.
- Bajer, A. S., Molè-Bajer, J.** (1986). Reorganization of microtubules in endosperm cells and cell fragments of the higher plant Haemanthus in vivo. *J. Cell Biol.* **102**(1), 263-81.
- Bakkaiova, J., Arata, K., Matsunobu, M., Ono, B., Aoki, T., Lajdova, D., Nebohacova, M., Nosek, J., Miyakawa, I., Tomaska, L.** (2014). The strictly aerobic yeast Yarrowia lipolytica tolerates loss of a mitochondrial DNA-packaging protein. *Eukaryot. Cell* **13**(9), 1143-57.
- Barboni, B., Russo, V., Cecconi, S., Curini, V., Colosimo, A., Garofalo, M. L., Capacchietti, G., Di Giacinto, O., Mattioli, M.** (2011). In vitro grown sheep preantral follicles yield oocytes with normal nuclear-epigenetic maturation. *PLoS One* **6**(11), e27550.
- Bischof, J., Brand, C. A., Somogyi, K., Májer, I., Thome, S., Mori, M., Schwarz, U. S., Lénárt, P.** (2017). A cdk1 gradient guides surface contraction waves in oocytes. *Nat. Commun.* **8**(1), 849.

- Blume, Y. B., Krasylenko, Y. A., Demchuk, O. M., Yemets, A. I.** (2013). Tubulin tyrosine nitration regulates microtubule organization in plant cells. *Front. Plant Sci.* **4**, 530.
- Bradley, J. T., Kloc, M., Wolfe, K. G., Estridge, B. H., Bilinski, S. M.** (2001). Balbiani bodies in cricket oocytes: development, ultrastructure, and presence of localized RNAs. *Differentiation*. **67(4-5)**, 117-27.
- Branco, I. S. L., Viana, D. L., Félix, R. T. S., Véras, D. P., Hazin, F. H. V.** (2013). Oocyte development and ovarian maturation of the black triggerfish, *Melichthys niger* (*Actinopterygii: Balistidae*) in São Pedro e São Paulo Archipelago, Brazil. *Neotrop. Ichthyol.* **11(3)**, 597-606.
- Brandt, A. et al.** (2006). Developmental control of nuclear size and shape by Kugelkern and Kurzkern. *Curr. Biol.* **16(6)**, 543-52.
- Burrows, A. E., Sceurman, B. K., Kosinski, M. E., Richie, C. T., Sadler, P. L., Schumacher, J. M., Golden, A.** (2006). The *C. elegans* Myt1 ortholog is required for the proper timing of oocyte maturation. *Development* **133(4)**, 697-709.
- Cabral, M., Anjard, C., Malhotra, V., Loomis, W. F., Kuspa, A.** (2010). Unconventional secretion of AcbA in *Dictyostelium discoideum* through a vesicular intermediate. *Eukaryot. Cell.* **9(7)**, 1009-17.
- Capuano, C. M., Grzesik, P., Kreitler, D., Pryce, E. N., Desai, K. V., Coombs, G., McCaffery, J. M., Desai, P. J.** (2014). A hydrophobic domain within the small capsid protein of Kaposi's sarcoma-associated herpesvirus is required for assembly. *J. Gen. Virol.* **95(Pt 8)**, 1755-69.
- Casco-Robles, R. M. et al.** (2018). Novel erythrocyte clumps revealed by an orphan gene Newticl in circulating blood and regenerating limbs of the adult newt. *Sci. Rep.* **8(1)**, 7455.
- Chang, T. C., Eddy, C. A., Ying, Y., Liu, Y. G., Holden, A. E., Brzyski, R. G., Schenken, R. S.** (2011). Ovarian stimulation, in vitro fertilization, and effects of culture conditions on baboon preimplantation embryo development. *Fertil. Steril.* **95(4)**, 1217-23.
- Chen, P. F., Singhal, S., Bushyhead, D., Broder-Fingert, S., Wolfe, J.** (2014). Colchicine-induced degeneration of the micronucleus during conjugation in *Tetrahymena*. *Biol. Open.* **3(5)**, 353-61.
- Chen, P., Tomschik, M., Nelson, K., Oakey, J., Gatlin, J. C., Levy, D. L.** (2019). Cytoplasmic volume and limiting nucleoplasmin scale nuclear size during *Xenopus laevis* development, *bioRxiv*, 511451.
- Chen, S., Liao, J., Luo, M., Kirchoff, B.** (2008). Calcium distribution and function during anther development of *Torenia fournieri* (Linderniaceae). *Annales Botanici Fennici*, **45(3)**, 195-203.

**Chen, X., Shen, Y., Ellis, R. E.** (2014). Dependence of the sperm/oocyte decision on the nucleosome remodeling factor complex was acquired during recent *Caenorhabditis briggsae* evolution. *Mol. Biol. Evol.* **31(10)**, 2573-85.

**Chérel, D., Beninger, P. G.** (2017). Oocyte Atresia Characteristics and Effect on Reproductive Effort of Manila Clam *Tapes philippinarum* (Adams and Reeve, 1850). *J. Shellfish Res.* **36(3)**, 549-557

**Chida, J., Yamaguchi, H., Amagai, A., Maeda, Y.** (2004). The necessity of mitochondrial genome DNA for normal development of Dictyostelium cells. *J. Cell Sci.* **117(Pt 15)**, 3141-52.

**Conklin, E. G.** (1912). Cell size and nuclear size. *J. Exp. Zool.* **12(1)**, 1-98.

**Consentino, L. et al.** (2015). Blue-light dependent reactive oxygen species formation by Arabidopsis cryptochrome may define a novel evolutionarily conserved signaling mechanism. *New Phytol.* **206(4)**, 1450-62.

**Conti, S. F., Naylor, H. B.** (1960). Electron microscopy of ultrathin sections of *Schizosaccharomyces octosporus*. III. Ascosporegenesis, ascospore structure, and germination. *J. Bacteriol.* **79**, 417-25.

**Cui, X., Guo, Z., Song, L., Wang, Y., Cheng, Y.** (2016). NCP1/AtMOB1A Plays Key Roles in Auxin-Mediated Arabidopsis Development. *PLoS Genet.* **12(3)**, e1005923.

**Danilchik, M. V., Gerhart, J. C.** (1987). Differentiation of the animal-vegetal axis in *Xenopus laevis* oocytes. I. Polarized intracellular translocation of platelets establishes the yolk gradient. *Dev. Biol.* **122(1)**, 101-12.

**Davison, M. T., Garland, P. B.** (1977). Structure of mitochondria and vacuoles of *Candida utilis* and *Schizosaccharomyces pombe* studied by electron microscopy of serial thin sections and model building. *J. Gen. Microbiol.* **98(1)**, 147-53

**Debowski, K., Drummer, C., Lentes, J., Cors, M., Dressel, R., Lingner, T., Salinas-Riester, G., Fuchs, S., Sasaki, E., Behr, R.** (2016). The transcriptomes of novel marmoset monkey embryonic stem cell lines reflect distinct genomic features. *Sci. Rep.* **6**, 29122.

**Delcros, J. G., Prigent, C., Giet, R.** (2006). Dynactin targets Pavarotti-KLP to the central spindle during anaphase and facilitates cytokinesis in Drosophila S2 cells. *J. Cell Sci.* **119(Pt 21)**, 4431-41.

**Denzel, S., Maetzel, D., Mack, B., Eggert, C., Bärr, G., Gires, O.** (2009). Initial activation of EpCAM cleavage via cell-to-cell contact. *BMC Cancer.* **9**, 402.

- Deparis, P., Jaylet, A.** (1984). The role of endoderm in blood cell ontogeny in the newt *Pleurodeles waltl*. *J. Embryol. Exp. Morphol.* **81**, 37-47.
- Dixon, D. R.** (1983). Methods for Assessing the Effects of Chemicals on Reproductive Function in Marine Molluscs. Methods Assess. In *Vouk, V.B. and Sheehan, P.J. eds. Methods for assessing the effects of chemicals on reproductive functions*, pp. 439–57. Chichester, UK: John Wiley.
- Dumolland, R., Gazo, I., Gomes, I. D. L., Besnardieu, L., McDougall, A.** (2017). Ascidians: An Emerging Marine Model for Drug Discovery and Screening. *Curr. Top. Med. Chem.* **17**(18), 2056-2066.
- Duncan, F. E., Padilla-Banks, E., Bernhardt, M. L., Ord, T. S., Jefferson, W. N., Moss, S. B., Williams, C. J.** (2014). Transducin-like enhancer of split-6 (TLE6) is a substrate of protein kinase A activity during mouse oocyte maturation. *Biol. Reprod.* **90**(3), 63.
- Eildermann, K. et al.** (2012). Developmental expression of the pluripotency factor sal-like protein 4 in the monkey, human and mouse testis: restriction to premeiotic germ cells. *Cells Tissues Organs*. **196**(3), 206-20.
- Elaasser, M., Magdi, H. M., Mourad, M. H., Ahmed, H. Y.** (2017). Fungal Detoxification of Certain Fusarium Moniliforme Mycotoxins Using *Yarrowia Lipolytica* with Special Emphasis on its Possible Mechanism of Action. *IOSR J. Pharma. Biol. Sci.* **12**, 63-73.
- Elkouby, Y. M., Jamieson-Lucy, A., Mullins, M. C.** (2016). Oocyte Polarization Is Coupled to the Chromosomal Bouquet, a Conserved Polarized Nuclear Configuration in Meiosis. *PLoS Biol.* **14**(1), e1002335.
- Ereskovsky, A. V.** (2010). *The Comparative Embryology of Sponges*. Springer, Dordrecht
- Faure, E. et al.** (2016). A workflow to process 3D+time microscopy images of developing organisms and reconstruct their cell lineage. *Nat. Commun.* **7**, 8674.
- Feng, X., Dickinson, H. G.** (2010). Tapetal cell fate, lineage and proliferation in the *Arabidopsis* anther. *Development*. **137**(14), 2409-16.
- Feric, M., Brangwynne, C. P.** (2013). A nuclear F-actin scaffold stabilizes ribonucleoprotein droplets against gravity in large cells. *Nat. Cell Biol.* **15**(10), 1253-9.
- Ferreira, A., Dolder, H.** (2003). Sperm ultrastructure and spermatogenesis in the lizard, *Tropidurus itambere*. *Biocell.* **27**(3), 353-62.
- Fields, S. D., Conrad, M. N., Clarke, M.** (1998). The *S. cerevisiae* CLU1 and *D. discoideum* cluA genes are functional homologues that influence mitochondrial morphology and distribution. *J. Cell Sci.* **111**(Pt 12), 1717-27.

- Fischer, A.** (1974). Stages and stage distribution in early oogenesis in the Annelid, *Platynereis dumerilii*. *Cell Tissue Res.* **156**(1), 35-45.
- Flament, S., Dumond, H., Chardard, D., Chesnel, A.** (2009). Lifelong testicular differentiation in *Pleurodeles waltl* (Amphibia, Caudata). *Reprod. Biol. Endocrinol.* **7**, 21.
- Frank, S. R., Köllmann, C. P., Luong, P., Galli, G. G., Zou, L., Bernards, A., Getz, G., Calogero, R. A., Frödin, M., Hansen, S. H.** (2018). p190 RhoGAP promotes contact inhibition in epithelial cells by repressing YAP activity. *J. Cell Biol.* **217**(9), 3183-3201.
- Fraser, H. M., Hastings, J. M., Allan, D., Morris, K. D., Rudge, J. S., Wiegand, S. J.** (2012). Inhibition of delta-like ligand 4 induces luteal hypervasculartization followed by functional and structural luteolysis in the primate ovary. *Endocrinology*, **153**(4), 1972-83.
- Fujioka, A., Terai, K., Itoh, R. E., Aoki, K., Nakamura, T., Kuroda, S., Nishida, E., Matsuda, M.** (2006). Dynamics of the Ras/ERK MAPK cascade as monitored by fluorescent probes. *J. Biol. Chem.* **281**(13), 8917-26.
- Fujiu, K., Numata, O.** (2000). Reorganization of microtubules in the amitotically dividing macronucleus of tetrahymena. *Cell Motil. Cytoskeleton.* **46**(1), 17-27.
- Galindo, L. J., Torruella, G., Moreira, D., Timpano, H., Paskerova, G., Smirnov, A., Nassonova, E., López-García, P.** (2018). Evolutionary Genomics of *Metchnikovella incurvata* (Metchnikovellidae): An Early Branching Microsporidium. *Genome Biol. Evol.* **10**(10), 2736-2748.
- Gall, J. G., Nizami, Z. F.** (2016). Isolation of Giant Lampbrush Chromosomes from Living Oocytes of Frogs and Salamanders. *J. Vis. Exp.* **5**, 118.
- Gallo, A., Russo, G. L., Tosti, E.** (2013). T-type Ca<sup>2+</sup> current activity during oocyte growth and maturation in the ascidian *Styela plicata*. *PLoS One.* **8**(1), e54604.
- Gao, J., Wallis, J. G., Jewell, J. B., Browne, J.** (2017). Trimethylguanosine Synthase1 (TGS1) Is Essential for Chilling Tolerance. *Plant Physiol.* **174**(3), 1713-1727.
- Garner, S., Zysk, I., Byrne, G., Kramer, M., Moller, D., Taylor, V., Burke, R. D.** (2016). Neurogenesis in sea urchin embryos and the diversity of deuterostome neurogenic mechanisms. *Development.* **143**(2), 286-97.
- Glowinski, C., Liu, R. H., Chen, X., Darabie, A., Godt, D.** (2014). Myosin VIIA regulates microvillus morphogenesis and interacts with cadherin Cad99C in Drosophila oogenesis. *J. Cell Sci.* **127**(Pt 22), 4821-32.
- Goud, P. T., Goud, A. P., Qian, C., Lavarge, H., Van der Elst, J., De Sutter, P., Dhont, M.** (1998). In-vitro maturation of human germinal vesicle stage oocytes: role of cumulus cells and epidermal growth factor in the culture medium. *Hum. Reprod.* **13**(6), 1638-44.

- Gould-Somero, M., Holland, L.** (1975). Oocyte differentiation in *Urechis caupo* (Echiura): a fine structural study. *J. Morphol.* **147**(4), 475-505.
- Gray, W. T., Govers, S. K., Xiang, Y., Parry, B. R., Campos, M., Kim, S., Jacobs-Wagner, C.** (2019). Nucleoid Size Scaling and Intracellular Organization of Translation across Bacteria. *Cell.* **177**(6), 1632-1648.e20.
- Gregory, T. R.** (2001). Coincidence, coevolution, or causation? DNA content, cell size, and the C-value enigma. *Biol. Rev. Camb. Philos. Soc.* **76**(1), 65-101.
- Gu, Y., Oliferenko, S.** (2019). Cellular geometry scaling ensures robust division site positioning. *Nat. Commun.* **10**(1), 268.
- Gunkel, K., van der Klei, I. J., Barth, G., Veenhuis, M.** (1999). Selective peroxisome degradation in *Yarrowia lipolytica* after a shift of cells from acetate/oleate/ethylamine into glucose/ammonium sulfate-containing media. *FEBS Lett.* **451**(1), 1-4.
- Han, Y., Liu, X. M., Liu, H., Li, S. C., Wu, B. C., Ye, L. L., Wang, Q. W., Chen, Z. L.** (2006). Cultivation of recombinant Chinese hamster ovary cells grown as suspended aggregates in stirred vessels. *J. Biosci. Bioeng.* **102**(5), 430-5.
- Hanna, C. B., Yao, S., Patta, M. C., Jensen, J. T., Wu, X.** (2010). WEE2 is an oocyte-specific meiosis inhibitor in rhesus macaque monkeys. *Biol. Reprod.* **82**(6), 1190-7.
- Hara, Y., Adachi, K., Kagohashi, S., Yamagata, K., Tanabe, H., Kikuchi, S., Okumura, S. I., Kimura, A.** (2016). Scaling relationship between intra-nuclear DNA density and chromosomal condensation in metazoan and plant. *Chromo. Sci.* **19**, 43-49.
- Hara, Y., Iwabuchi, M., Ohsumi, K., Kimura, A.** (2013). Intranuclear DNA density affects chromosome condensation in metazoans. *Mol. Biol. Cell.* **24**(15), 2442-53.
- Hara, Y., Kimura, A.** (2009). Cell-size-dependent spindle elongation in the *Caenorhabditis elegans* early embryo. *Curr. Biol.* **19**(18), 1549-54.
- Hayes, M. H., Weeks, D. L.** (2016). Amyloids assemble as part of recognizable structures during oogenesis in *Xenopus*. *Biol. Open.* **5**(6), 801-6.
- Heger, P., Kroher, M., Ndifon, N., Schierenberg, E.** (2010). Conservation of MAP kinase activity and MSP genes in parthenogenetic nematodes. *BMC Dev. Biol.* **10**, 51.
- Hiebert, T. C., Maslakova, S. A.** (2015). Larval Development of Two N. E. Pacific *Pilidiophoran Nemerteans* (Heteronemertea; Lineidae). *Biol. Bull.* **229**(3), 265-75.
- Hildreth, S. B. et al.** (2011). Tobacco nicotine uptake permease (NUP1) affects alkaloid metabolism. *Proc. Natl. Acad. Sci. USA.* **108**(44), 18179-84.
- Hiwatashi, Y., Obara, M., Sato, Y., Fujita, T., Murata, T., Hasebe, M.** (2008). Kinesins are indispensable for interdigititation of phragmoplast microtubules in the moss *Physcomitrella patens*. *Plant Cell.* **20**(11), 3094-106.

**Holland, N. D., Giese, A. C.** (1965). An Autoradiographic Investigation of the Gonads of the Purple Sea Urchin (*Strongylocentrotus purpuratus*). *Biological Bulletin*. **128**(2), 241-258.

**Hou, M., Chrysis, D., Nurmi, M., Parvinen, M., Eksborg, S., Söder, O., Jahnukainen, K.** (2005). Doxorubicin induces apoptosis in germ line stem cells in the immature rat testis and amifostine cannot protect against this cytotoxicity. *Cancer Res.* **65**(21), 9999-10005.

<http://www.echinobase.org/Echinobase/>

<https://vcbio.science.ru.nl/>

**Imoh, H.** (1982). Behaviour of annulate lamellae during the maturation of oocytes in the newt, *Cynops pyrrhogaster*. *J. Embryol. Exp. Morphol.* **70**, 153-69.

**Inoue, T., Iida, A., Maegawa, S., Sehara-Fujisawa, A., Kinoshita, M.** (2016). Generation of a transgenic medaka (*Oryzias latipes*) strain for visualization of nuclear dynamics in early developmental stages. *Dev. Growth Differ.* **58**(9), 679-687.

**Ishida, M., Hori, M.** (2017). Improved isolation method to establish axenic strains of Paramecium. *J. Protistol.* **50**, 1-14.

**Iwamoto, M., Mori, C., Kojidani, T., Bunai, F., Hori, T., Fukagawa, T., Hiraoka, Y., Haraguchi, T.** (2009). Two distinct repeat sequences of Nup98 nucleoporins characterize dual nuclei in the binucleated ciliate tetrahymena. *Curr. Biol.* **19**(10), 843-7.

**Jammes, F.** (2009). MAP kinases MPK9 and MPK12 are preferentially expressed in guard cells and positively regulate ROS-mediated ABA signaling. *Proc. Natl. Acad. Sci. USA.* **106**(48), 20520-5.

**Jevtić, P., Levy, D. L.** (2015). Nuclear size scaling during *Xenopus* early development contributes to midblastula transition timing. *Curr. Biol.* **25**(1), 45-52.

**Jiang, Y. Y., Maier, W., Baumeister, R., Minevich, G., Joachimiak, E., Ruan, Z., Kannan, N., Clarke, D., Frankel, J., Gaertig, J.** (2017). The Hippo Pathway Maintains the Equatorial Division Plane in the Ciliate Tetrahymena. *Genetics*. **206**(2), 873-888.

**Jiao, G. Z., Cui, W., Yang, R., Lin, J., Gong, S., Lian, H. Y., Sun, M. J., Tan, J. H.** (2016). Optimized Protocols for In Vitro Maturation of Rat Oocytes Dramatically Improve Their Developmental Competence to a Level Similar to That of Ovulated Oocytes. *Cell Reprogram.* **18**(1), 17-29.

**Jorgensen, P., Edgington, N. P., Schneider, B. L., Rupes, I., Tyers, M., Futcher, B.** (2007). The size of the nucleus increases as yeast cells grow. *Mol. Biol. Cell.* **18**(9), 3523-3532.

**Julaton, V. T., Reijo Pera, R. A.** (2011). NANOS3 function in human germ cell development. *Hum. Mol. Genet.* **20**(11), 2238-50.

**Kakiuchi, K., Taniguchi, K., Kubota, H.** (2018). Conserved and non-conserved characteristics of porcine glial cell line-derived neurotrophic factor expressed in the testis. *Sci. Rep.* **8**(1), 7656.

**Kai, Y., Moriwaki, H., Yumoto, K., Iwata, K., Mio, Y.** (2018). Assessment of developmental potential of human single pronucleated zygotes derived from conventional in vitro fertilization. *J. Assist. Reprod. Genet.* **35**(8), 1377-1384.

**Kimata, Y., Higaki, T., Kawashima, T., Kurihara, D., Sato, Y., Yamada, T., Hasezawa, S., Berger, F., Higashiyama, T., Ueda, M.** (2016). Cytoskeleton dynamics control the first asymmetric cell division in *Arabidopsis* zygote. *Proc. Natl. Acad. Sci. USA.* **113**(49), 14157-14162.

**Kiyomoto, M., Hamanaka, G., Hirose, M., Yamaguchi, M.** (2013). Preserved echinoderm gametes as a useful and ready-to-use bioassay material. *Mar. Environ. Res.* **93**, 102-5.

**Kominami, T.** (1983). Establishment of embryonic axes in larvae of the starfish, *Asterina pectinifera*. *J. Embryol. Exp. Morphol.* **75**, 87-100.

**Kominami, T., Takata, H.** (2003). Timing of early developmental events in embryos of a tropical sea urchin *Echinometra mathaei*. *Zool. Sci.* **20**(5), 617-26.

**Krasikova, A., Khodyuchenko, T., Maslova, A., Vasilevskaya, E.** (2012). Three-dimensional organisation of RNA-processing machinery in avian growing oocyte nucleus. *Chromo. Res.* **20**(8), 979-94.

**Kraus, C., Schiffer, P. H., Kagoshima, H., Hiraki, H., Vogt, T., Kroher, M., Kohara, Y., Schierenberg, E.** (2017). Differences in the genetic control of early egg development and reproduction between *C. elegans* and its parthenogenetic relative *D. coronatus*. *Evodevo.* **8**, 16.

**Kryuchkova, M., Danilushkina, A., Lvovab, Y., Fakhrullin, R.** (2016). Evaluation of toxicity of nanoclays and graphene oxide in vivo: a *Paramecium caudatum* study. *Environ. Sci.: Nano.* **3**, 442-452.

**Kume, K., Cantwell, H., Neumann, F. R., Jones, A. W., Snijders, A. P., Nurse, P.** (2017). A systematic genomic screen implicates nucleocytoplasmic transport and membrane growth in nuclear size control. *PLoS Genet.* **13**(5), e1006767.

**Kurusu, T., Saito, K., Horikoshi, S., Hanamata, S., Negi, J., Yagi, C., Kitahata, N., Iba, K., Kuchitsu, K.** (2013). An S-type anion channel SLAC1 is involved in cryptogein-induced ion fluxes and modulates hypersensitive responses in tobacco BY-2 cells. *PLoS One.* **8**(8), e70623.

**Kyogoku, H., Fulka, J. Jr, Wakayama, T., Miyano, T.** (2014). De novo formation of nucleoli in developing mouse embryos originating from enucleolated zygotes. *Development.* **141**(11), 2255-9.

**Le Goff, E., Martinand-Mari, C., Martin, M., Feuillard, J., Boublik, Y., Godefroy, N., Mangeat, P., Baghdiguian, S., Cavalli, G.** (2015). Enhancer of zeste acts as a major developmental regulator of *Ciona intestinalis* embryogenesis. *Biol. Open.* **4**(9), 1109-21.

**Lee, K. H., Yamaguchi, A., Rashid, H., Kadomura, K., Yasumoto, S., Matsuyama, M.** (2009). Estradiol-17beta treatment induces intersexual gonadal development in the pufferfish, *Takifugu rubripes*. *Zool. Sci.* **26**(9), 639-45.

**Leitch, H. G., Blair, K., Mansfield, W., Ayetey, H., Humphreys, P., Nichols, J., Surani, M. A., Smith, A.** (2010). Embryonic germ cells from mice and rats exhibit properties consistent with a generic pluripotent ground state. *Development.* **137**(14), 2279-87.

**Léonet, A., Rasolofonirina, R., Wattiez, R., Jangoux, M., Eeckhaut, I.** (2009). A new method to induce oocyte maturation in holothuroids (Echinodermata). *Invert. Reprod. Dev.* **53**, 13-21.

**Levy, D. L., Heald, R.** (2010). Nuclear size is regulated by importin  $\alpha$  and Ntf2 in *Xenopus*. *Cell.* **143**(2), 288-98.

**Li, C., Yue, J., Wu, X., Xu, C., Yu, J.** (2014). An ABA-responsive DRE-binding protein gene from *Setaria italica*, SiARDP, the target gene of SiAREB, plays a critical role under drought stress. *J. Exp. Bot.* **65**(18), 5415-27.

**Li, J., Chu, H., Zhang, Y., Mou, T., Wu, C., Zhang, Q., Xu, J.** (2012). The rice HGW gene encodes a ubiquitin-associated (UBA) domain protein that regulates heading date and grain weight. *PLoS One.* **7**(3), e34231.

**Li, J., Dong, Y., Li, C., Pan, Y., Yu, J.** (2017). SiASR4, the Target Gene of SiARDP from *Setaria italica*, Improves Abiotic Stress Adaption in Plants. *Front. Plant Sci.* **7**, 2053.

**Lindeman, R. E., Pelegri, F.** (2012). Localized products of futile cycle/lrmp promote centrosome-nucleus attachment in the zebrafish zygote. *Curr. Biol.* **22**(10), 843-51.

**Liu, H. J., Liu, R. M.** (2018). Dynamic changes in chromatin and microtubules at the first cell cycle in SCNT or IVF goat embryos. *Cell Biol. Int.* **42**(10), 1401-1409.

**Liu, X. Q., Liu, Z. Q., Yu, C. Y., Dong, J. G., Hu, S. W., Xu, A. X.** (2017). TGMS in Rapeseed (*Brassica napus*) Resulted in Aberrant Transcriptional Regulation, Asynchronous Microsporocyte Meiosis, Defective Tapetum, and Fused Sexine. *Front. Plant Sci.* **8**, 1268.

**Lubzens, E., Young, G., Bobe, J., Cerdà, J.** (2010). Oogenesis in teleosts: how eggs are formed. *Gen. Comp. Endocrinol.* **165**(3), 367-89.

**Ludwig-Müller, J., Jülke, S., Bierfreund, N. M., Decker, E. L., Reski, R.** (2009). Moss (*Physcomitrella patens*) GH3 proteins act in auxin homeostasis. *New Phytol.* **181**(2), 323-338.

**Lung, S. C., Yanagisawa, M., Chuong, S. D.** (2011). Protoplast isolation and transient gene expression in the single-cell C4 species, *Bienertia sinuspersici*. *Plant Cell Rep.* **30**(4), 473-84.

**Lyons, D. C., Perry, K. J., Henry, J. Q.** (2015). Spiralian gastrulation: germ layer formation, morphogenesis, and fate of the blastopore in the slipper snail *Crepidula fornicate*. *Evodevo*. **6**, 24.

**Ma, F. et al.** (2008). Direct development of functionally mature tryptase/chymase double-positive connective tissue-type mast cells from primate embryonic stem cells. *Stem Cells*. **26**(3), 706-14.

**Maekawa, H., Neuner, A., Rüthnick, D., Schiebel, E., Pereira, G., Kaneko, Y.** (2017). Polo-like kinase Cdc5 regulates Spc72 recruitment to spindle pole body in the methylotrophic yeast *Ogataea polymorpha*. *Elife*. **6**, e24340.

**Mak, D. O., Vais, H., Cheung, K. H., Foskett, J. K.** (2013). Isolating nuclei from cultured cells for patch-clamp electrophysiology of intracellular Ca(2+) channels. *Cold Spring Harb. Protoc.* **2013**(9), 880-4.

**Malik, J., Lillis, J. A., Couch, T., Getman, M., Steiner, L. A.** (2017). The Methyltransferase Setd8 Is Essential for Erythroblast Survival and Maturation. *Cell Rep.* **21**(9), 2376-2383.

**Masuda, K., Xu, Z. J., Takahashi, S., Ito, A., Ono, M., Nomura, K., Inoue, M.** (1997). Peripheral framework of carrot cell nucleus contains a novel protein predicted to exhibit a long alpha-helical domain. *Exp. Cell Res.* **232**(1), 173-81.

**Maul, G. G., Deaven, L.** (1977). Quantitative determination of nuclear pore complexes in cycling cells with differing DNA content. *J. Cell Biol.* **73**(3), 748-60.

**McDougall, A., Hebras, C., Pruliere, G., Burgess, D., Costache, V., Dumollard, R., Chenevert, J.** (2017). Role of midbody remnant in meiosis II creating tethered polar bodies. *bioRxiv*, 191981.

**Meckel, T., Gall, L., Semrau, S., Homann, U., Thiel, G.** (2007). Guard cells elongate: relationship of volume and surface area during stomatal movement. *Biophys. J.* **92**(3), 1072-80.

**Miranda-Rodríguez, J. R., Salas-Vidal, E., Lomelí, H., Zurita, M., Schnabel, D.** (2017). RhoA/ROCK pathway activity is essential for the correct localization of the germ plasm mRNAs in zebrafish embryos. *Dev. Biol.* **421**(1), 27-42.

**Misumi, O., Matsuzaki, M., Nozaki, H., Miyagishima, S. Y., Mori, T., Nishida, K., Yagisawa, F., Yoshida, Y., Kuroiwa, H., Kuroiwa, T.** (2005). *Cyanidioschyzon merolae* genome. A tool for facilitating comparable studies on organelle biogenesis in photosynthetic eukaryotes. *Plant Physiol.* **137**(2), 567-85.

**Moiseeva, E., Rabinowitz, C., Paz, G., Rinkevich, B.** (2017). Histological study on maturation, fertilization and the state of gonadal region following spawning in the model sea anemone, *Nematostella vectensis*. *PLoS One*. **12**(8), e0182677.

**Money, N. P.** (2016). Chapter 12 - Fungi and Biotechnology, *The Fungi (Third Edition)*, 401–424.

**Mueller, R. L., Gregory, T. R., Gregory, S. M., Hsieh, A., Boore, J. L.** (2008). Genome size, cell size, and the evolution of enucleated erythrocytes in attenuate salamanders. *Zoology (Jena)*. **111**(3), :218-30.

**Neumann, F. R., Nurse, P.** (2007). Nuclear size control in fission yeast. *J. Cell Biol.* **179**(4), 593-600.

**Niehoff, B.** (1998). The gonad morphology and maturation in Arctic *Calanus* species. *J. Marine Sys.* **15**, 53-59.

**Nodine, M. D., Bartel, D. P.** (2010). MicroRNAs prevent precocious gene expression and enable pattern formation during plant embryogenesis. *Genes Dev.* **24**(23), 2678-92.

**Noorafshan, A., Motamedifar, M., Karbalay-Doust, S.** (2016). Estimation of the Cultured Cells' Volume and Surface Area: Application of Stereological Methods on Vero Cells Infected by Rubella Virus. *Iran J. Med. Sci.* **41**(1), 37-43.

**Novakova, L., Kovacovicova1 K., Dang-Nguyen, T. Q., Sodek, M., Skultety, M., Anger, M.** (2016). A Balance between Nuclear and Cytoplasmic Volumes Controls Spindle Length. *PLoS ONE.* **11**(2), e0149535.

**Oberlender, G., Ruiz López, S., De Ondiz Sánchez, A. D., Vieira, L. A., Pereira, M. B., Silva, L. F., Zangeronimo, M. G., Murgas, L. D. S.** (2016). In vitro fertilization of porcine oocytes is affected by spermatic coincubation time. *Pesq. Vet. Bras.* **36**(Supl.1), 58-64.

**O'Donnell, L., Narula, A., Balourdos, G., Gu, Y. Q., Wreford, N. G., Robertson, D. M., Bremner, W. J., McLachlan, R. I.** (2001). Impairment of spermatogonial development and spermiation after testosterone-induced gonadotropin suppression in adult monkeys (*Macaca fascicularis*). *J. Clin. Endocrinol. Metab.* **86**(4), 1814-22.

**Ogonuki, N., Tsuchiya, H., Hirose, Y., Okada, H., Ogura, A., Sankai, T.** (2003). Pregnancy by the tubal transfer of embryos developed after injection of round spermatids into oocyte cytoplasm of the cynomolgus monkey (*Macaca fascicularis*). *Hum. Reprod.* **18**(6), 1273-80.

**Ondracka, A., Dudin, O., Ruiz-Trillo, I.** (2018). Decoupling of Nuclear Division Cycles and Cell Size during the Coenocytic Growth of the Ichthyosporean *Sphaeroforma arctica*. *Curr. Biol.* **28**(12), 1964-1969.e2.

**Oulhen, N., Onorato, T. M., Ramos, I., Wessel, G. M.** (2014). Dysferlin is essential for endocytosis in the sea star oocyte. *Dev. Biol.* **388**(1), 94-102.

**Payne, T. M., Molestina, R. E., Sinai, A. P.** (2003). Inhibition of caspase activation and a requirement for NF-kappaB function in the Toxoplasma gondii-mediated blockade of host apoptosis. *J. Cell Sci.* **116**(Pt 21), 4345-58.

- Peng, C. J., Wikramanayake, A. H.** (2013). Differential regulation of disheveled in a novel vegetal cortical domain in sea urchin eggs and embryos: implications for the localized activation of canonical Wnt signaling. *PLoS One.* **8(11)**, e80693.
- Piras, A. R. et al.** (2018). Structure of preantral follicles, oxidative status and developmental competence of in vitro matured oocytes after ovary storage at 4 °C in the domestic cat model. *Reprod. Biol. Endocrinol.* **16(1)**, 76.
- Pires, A., Gentil, F., Quintino, V., Rodrigues, A. M.** (2011). Reproductive biology of *Diopatra neapolitana* (Annelida, Onuphidae), an exploited natural resource in Ria de Aveiro (Northwestern Portugal). *Marine Ecology.* **33**, 56-65.
- Pires, E. S.** (2015). Consider Anti-Ovarian Antibody Testing for ART: a Parameter to Improve the Success Rate of Your Clinic! Austin J. *In Vitro Fertil.* **2(3)**, 1022.
- Pouthas, F., Girard, P., Lecaudey, V., Ly, T. B., Gilmour, D., Boulin, C., Pepperkok, R., Reynaud, E. G.** (2008). In migrating cells, the Golgi complex and the position of the centrosome depend on geometrical constraints of the substratum. *J. Cell Sci.* **121(Pt 14)**, 2406-14.
- Price, H. J., Sparrow, A. H., Nauman, F.** (1973). Correlations between nuclear volume, cell volume and DNA content in meristematic cells of herbaceous angiosperms. *Experientia.* **239(8)**, 1028-1029.
- Prodon, F., Chenevert, J., Sardet, C.** (2006). Establishment of animal-vegetal polarity during maturation in ascidian oocytes. *Dev. Biol.* **290(2)**, 297-311.
- Ramos-Miranda, J. et al.** (2017). Reproductive cycle of the sea cucumber *Holothuria floridana* in the littorals of Campeche, Mexico. *Fisheries Sci.* **83(5)**, 699-714.
- Reynaud, K., Fontbonne, A., Marseloo, N., Thoumire, S., Chebrout, M., de Lesegno, C. V., Chistant-Maillard, S.** (2005). In vivo meiotic resumption, fertilization and early embryonic development in the bitch. *Reproduction.* **130(2)**, 193-201.
- Rice, E. A. et al.** (2014). Expression of a truncated ATHB17 protein in maize increases ear weight at silking. *PLoS One.* **9(4)**, e94238.
- Rosenbluth, M. J., Lam, W. A., Fletcher, D. A.** (2006). Force microscopy of nonadherent cells: a comparison of leukemia cell deformability. *Biophys. J.* **90(8)**, 2994-3003.
- Rudel, D., Riebesell, M., Sommer, R. J.** (2005). Gonadogenesis in *Pristionchus pacificus* and organ evolution: development, adult morphology and cell-cell interactions in the hermaphrodite gonad. *Dev. Biol.* **277(1)**, 200-21.
- Saraya, R., Krikken, A. M., Veenhuis, M., van der Klei, I. J.** (2011). Peroxisome reintroduction in *Hansenula polymorpha* requires Pex25 and Rho1. *J. Cell Biol.* **193(5)**, 885-900.

**Sato, M., Nishikawa, T., Kajitani, H., Kawano, S.** (2007). Conserved relationship between FtsZ and peptidoglycan in the cyanelles of *Cyanophora paradoxa* similar to that in bacterial cell division. *Planta*. **227**(1), 177-87.

**Sayed, A. E. H., Ismail, R. F., Mitani, H.** (2018a). Oocyte atresia in WT (HdrR) and P53 (-/-) medaka (*Oryzias latipes*) exposed to UVA. *J. Photochem. Photobiol. B*. **183**, 57-63.

**Sayed, A. E. H., Kataoka, C., Oda, S., Kashiwada, S., Mitani, H.** (2018b). Sensitivity of medaka (*Oryzias latipes*) to 4-nonylphenol subacute exposure; erythrocyte alterations and apoptosis. *Environ. Toxicol. Pharmacol.* **58**, 98-104.

**Schnackenberg, B. J., Marzluff, W. F.** (2002). Novel localization and possible functions of cyclin E in early sea urchin development. *J. Cell Sci.* **115**(Pt 1), 113-21.

**Segonzac, C., Boyer, J. C., Ipotesi, E., Szponarski, W., Tillard, P., Touraine, B., Sommerer, N., Rossignol, M., Gibrat, R.** (2007). Nitrate efflux at the root plasma membrane: identification of an *Arabidopsis* excretion transporter. *Plant Cell*. **19**(11), 3760-77.

**Seike, T., Shimoda, C., Niki, H.** (2019). Asymmetric diversification of mating pheromones in fission yeast. *PLoS Biol.* **17**(1), e3000101.

**Seltzer, V., Pawlowski, T., Evrard, J. L., Canaday, J., Herzog, E., Schmit, A. C.** (2008). Plant Gamma-Tusc-Like Components: Their Role In Microtubule Nucleation. In: Blume Y.B., Baird W.V., Yemets A.I., Breviario D. (eds) *The Plant Cytoskeleton: a Key Tool for Agro-Biotechnology. NATO Science for Peace and Security Series C: Environmental Security*. Springer, Dordrecht pp. 3-22.

**Shang, Y., Li, B., Gorovsky, M. A.** (2002). *Tetrahymena thermophila* contains a conventional gamma-tubulin that is differentially required for the maintenance of different microtubule-organizing centers. *J. Cell Biol.* **158**(7), 1195-206.

**Shi, B., Liu, X., Xu, Y., Wang, S.** (2015). Molecular characterization of three gonadotropin subunits and their expression patterns during ovarian maturation in *Cynoglossus semilaevis*. *Int. J. Mol. Sci.* **16**(2), 2767-93.

**Short, K. W., Carpenter, S., Freyer, J. P., Mourant, J. R.** (2005). Raman spectroscopy detects biochemical changes due to proliferation in mammalian cell cultures. *Biophys. J.* **88**(6), 4274-88.

**Siegmund, L., Burmester, A., Fischer, M. S., Wöstemeyer, J.** (2013). A model for endosymbiosis: interaction between *Tetrahymena pyriformis* and *Escherichia coli*. *Eur. J. Protistol.* **49**(4), 552-63.

**Silk, A. D., Holland, A. J., Cleveland, D. W.** (2009). Requirements for NuMA in maintenance and establishment of mammalian spindle poles. *J. Cell Biol.* **184**(5), 677-90.

**Silva, G. M. et al.** (2015). In vitro development of secondary follicles from pre-pubertal and adult goats. *Zygote*. **23**(4), 475-84.

**Silvestre, F., Cuomo, A., Tosti, E.** (2009). Ion current activity and molecules modulating maturation and growth stages of ascidian (*Ciona intestinalis*) oocytes. *Mol. Reprod. Dev.* **76**(11), 1084-93.

**Simerly, C. R. et al.** (2010). Assisted Reproductive Technologies (ART) with baboons generate live offspring: a nonhuman primate model for ART and reproductive sciences. *Reprod. Sci.* **17**(10), 917-30.

**Sreenivas, D., Kaladhar, D. S. V. G. K., Yarla, N. S., Thomas, V. M., PalniSamy, A., Vadlapudi, V. R., Preethi, R.** (2014). In Vitro Production of Sheep Embryos in CR1aa Medium Supplemented with L-Ascorbic Acid. *J. Tissue Sci. Eng.* **5**, 131.

**Stricker, S. A., Cline, C., Goodrich, D.** (2013). Oocyte maturation and fertilization in marine nemertean worms: using similar sorts of signaling pathways as in mammals, but often with differing results. *Biol. Bull.* **224**(3), 137-55.

**Stricker, S. A., Smythe, T. L.** (2000). Multiple triggers of oocyte maturation in nemertean worms: the roles of calcium and serotonin. *J. Exp. Zool.* **287**(3), 243-61.

**Svoboda, O., Bartunek, P.** (2015). Origins of the Vertebrate Erythro/Megakaryocytic System. *Biomed. Res. Int.* **2015**, 632171.

**Tamori, Y., Iwai, T., Mita, K., Wakahara, M.** (2004). Spatio-temporal expression of a DAZ-like gene in the Japanese newt *Cynops pyrrhogaster* that has no germ plasm. *Dev. Genes Evol.* **214**(12), 615-27.

**Tsichlaki, E., FitzHarris, G.** (2016). Nucleus downscaling in mouse embryos is regulated by cooperative developmental and geometric programs. *Sci. Rep.* **6**, 28040.

**Tůmová, L., Petr, J., Žalmanová, T., Chmelíková, E., Kott, T., Tichovská, H., Kučerová-Chrpová, V., Hošková, K., Jílek, F.** (2013). Calcineurin expression and localisation during porcine oocyte growth and meiotic maturation. *Anim. Reprod. Sci.* **141**(3-4), 154-63.

**Uchida, M., McDermott, G., Wetzler, M., Le Gros, M. A., Myllys, M., Knoechel, C., Barron, A. E., Larabell, C. A.** (2009). Soft X-ray tomography of phenotypic switching and the cellular response to antifungal peptoids in *Candida albicans*. *Proc. Natl. Acad. Sci. USA.* **106**(46), 19375-80.

**Ueno, S., Ueno, T., Iwao, Y.** (2011). Role of the PI3K-TOR-S6K pathway in the onset of cell cycle elongation during *Xenopus* early embryogenesis. *Dev. Growth Differ.* **53**(8), 924-33.

**Umezawa, T., Kato, A., Ogoshi, M., Ookata, K., Munakata, K., Yamamoto, Y., Islam, Z., Doi, H., Romero, M. F., Hirose, S.** (2010). O<sub>2</sub>-filled swimbladder employs monocarboxylate transporters for the generation of O<sub>2</sub> by lactate-induced root effect hemoglobin. *PLoS One.* **7**(4), e34579.

**Uppaluri, S., Weber, S. C., Brangwynne, C. P.** (2016). Hierarchical Size Scaling during Multicellular Growth and Development. *Cell Rep.* **17(2)**, 345-352.

**Vávra, J., Hyliš, M., Fiala, I., Sacherová, V., Vossbrinck, C. R.** (2017). Microsporidian genus *Berwaldia* (Opisthosporidia, Microsporidia), infecting daphnids (Crustacea, Branchiopoda): Biology, structure, molecular phylogeny and description of two new species. *Eur. J. Protistol.* **61(Pt A)**, 1-12.

**Velasquez, S., Malik, S., Lutz, S. E., Scemes, E., Eugenin, E. A.** (2016). Pannexin1 Channels Are Required for Chemokine-Mediated Migration of CD4+ T Lymphocytes: Role in Inflammation and Experimental Autoimmune Encephalomyelitis. *J. Immunol.* **196(10)**, 4338-47.

**Viaris de Lesegno, C., Reynaud, K., Pechoux, C., Chebrout, M., Chastant-Maillard, S.** (2008). Ultrastructural evaluation of in vitro-matured canine oocytes. *Reprod. Fertil. Dev.* **20(5)**, 626-39.

**Vigneault, C., McGraw, S., Sirard, M. A.** (2009). Spatiotemporal expression of transcriptional regulators in concert with the maternal-to-embryonic transition during bovine in vitro embryogenesis. *Reproduction.* **137(1)**, 13-21.

**Vítová, M., Hendrychová, J., Cepák, V., Zachleder, V.** (2005). Visualization of DNA-containing structures in various species of *Chlorophyta*, *Rhodophyta* and *Cyanophyta* using SYBR Green I dye. *Folia. Microbiol. (Praha).* **50(4)**, 333-40.

**Waki, K., Imai, K. S., Satou, Y.** (2015). Genetic pathways for differentiation of the peripheral nervous system in ascidians. *Nat. Commun.* **6**, 8719.

**Walters, A. D., Amoateng, K., Wang, R., Chen, J. H., McDermott, G., Larabell, C. A., Gadál, O., Cohen-Fix, O.** (2019). Nuclear envelope expansion in budding yeast is independent of cell growth and does not determine nuclear volume. *Mol. Biol. Cell.* **30(1)**, 131-145.

**Wang, M., Bond, N. J., Letcher, A. J., Richardson, J. P., Lilley, K. S., Irvine, R. F., Clarke, J. H.** (2010). Genomic tagging reveals a random association of endogenous PtdIns5P 4-kinases IIalpha and IIbeta and a partial nuclear localization of the IIalpha isoform. *Biochem. J.* **430(2)**, 215-21.

**Wessel, G. M., Conner, S. D., Berg, L.** (2002). Cortical granule translocation is microfilament mediated and linked to meiotic maturation in the sea urchin oocyte. *Development.* **129(18)**, 4315-25.

*Wikibooks, IGCSE Science/Section 2: Structures and functions in living organisms*

**Wildner, D. D., Grier, H., Quagio-Grassiotto, I.** (2012). Female germ cell renewal during the annual reproductive cycle in Ostariophysians fish. *Theriogenology.* **79(4)**, 709-24.

**Xu, H., Lim, M., Dwarakanath, M., Hong, Y.** (2014). Vasa identifies germ cells and critical stages of oogenesis in the Asian seabass. *Int. J. Biol. Sci.* **10**(2), 225-35.

**Xu, M., Fazleabas, A. T., Shikanov, A., Jackson, E., Barrett, S. L., Hirshfeld-Cytron, J., Kiesewetter, S. E., Shea, L. D., Woodruff, T. K.** (2011). In vitro oocyte maturation and preantral follicle culture from the luteal-phase baboon ovary produce mature oocytes. *Biol. Reprod.* **84**(4), 689-97.

**Yadav, V., Sanyal, K.** (2018). Sad1 Spatiotemporally Regulates Kinetochore Clustering To Ensure High-Fidelity Chromosome Segregation in the Human Fungal Pathogen *Cryptococcus neoformans*. *mSphere*. **3**(4), e00190-18.

**Yam, C., Gu, Y., Oliferenko, S.** (2013). Partitioning and remodeling of the *Schizosaccharomyces japonicus* mitotic nucleus require chromosome tethers. *Curr. Biol.* **23**(22), 2303-2310.

**Yamada, M., Goshima, G.** (2017). Mitotic Spindle Assembly in Land Plants: Molecules and Mechanisms. *Biology (Basel)*. **6**(1), E6.

**Yamaguchi, M., Mori, Y., Kozuka, Y., Okada, H., Uematsu, K., Tame, A., Furukawa, H., Maruyama, T., Worman, C. O., Yokoyama, K.** (2012). Prokaryote or eukaryote? A unique microorganism from the deep sea. *J. Electron. Microsc. (Tokyo)*. **61**(6), 423-31.

**Yang, J., Yang, S., Beaujean, N., Niu, Y., He, X., Xie, Y., Tang, X., Wang, L., Zhou, Q., Ji, W.** (2007). Epigenetic marks in cloned rhesus monkey embryos: comparison with counterparts produced in vitro. *Biol. Reprod.* **76**(1), 36-42.

**Yazaki, I., Tsurugaya, T., Santella, L., Chun, J. T., Amore, G., Kusunoki, S., Asada, A., Togo, T., Akasaka, K.** (2015). Ca<sup>2+</sup> influx-linked protein kinase C activity regulates the β-catenin localization, micromere induction signalling and the oral-aboral axis formation in early sea urchin embryos. *Zygote*. **23**(3), 426-46.

**Zdravkovic, T, et al.** (2015). Human stem cells from single blastomeres reveal pathways of embryonic or trophoblast fate specification. *Development*. **142**(23), 4010-25.

**Zhang, Y. Z., Ouyang, Y. C., Hou, Y., Schatten, H., Chen, D. Y., Sun, Q. Y.** (2008). Mitochondrial behavior during oogenesis in zebrafish: a confocal microscopy analysis. *Dev. Growth Differ.* **50**(3), 189-201.

**Zwart, K. B., Harder, W.** (1983). Regulation of the Metabolism of Some Alkylated Amines in the Yeasts *Candida utilis* and *Hansenula polymorpha*. *J. Gen. Microbiol.* **129**, 3157–3169.

**Zwart, K. B., Veenhuis, M., Harder, W.** (1983). Significance of yeast peroxisomes in the metabolism of choline and ethanolamine. *Antonie Van Leeuwenhoek*. **49**(4-5), 369-85.